2018

An investigation of Onychophora (velvet worms) of the Illawarra region

C Chapman

An investigation of Onychophora (velvet worms) of the Illawarra region

Abstract

Onychophorans are a fascinating phylum of terrestrial invertebrates that form a group with the Arthropoda and Tardigrada known as Panarthropoda (Campbell *et al*. 2011). Diversity among the Onychophora has been grossly underestimated as their conserved morphology results in the prevalence of cryptic species, whereby two or more species may be grouped under one species name if gross morphology alone has been used as the only means of identification. In recent years, more detailed morphological analyses and the application of molecular analyses has shed more light on diversity among the Onychophora. Within this phylum, two families have been recognised, the Peripatopsidae and Peripatidae, with a lack of any higher taxonomic ranks. The family Peripatopsidae are found in Australia, New Zealand, South Africa, and New Guinea and currently consists of many monotypic genera. One of these, *Anoplokaros,* with its single species *Anoplokaros keerensis* Reid, 1996, was originally suggested to comprise a likely cryptic species-complex (Reid 1996). This hypothesis was tested within this study, employing an integrative taxonomic approach, involving both molecular and morphological analyses. It was revealed that three putative novel species are present within the Illawarra region, that were previously believed to be populations of *A. keerensis.* Unique morphological characters were observed in most of the populations examined, although these were not necessarily congruent with the mtDNA COI sequences. Morphological descriptions were also prepared for additional specimens that were not included in the phylogenetic analyses that could be used as a baseline to facilitate future revisions of these putative *A. keerensis* populations.

Degree Type

Thesis

Degree Name

BEnviSci Hons

Department

School of Earth & Environmental Sciences

Advisor(s)

James Wallman

Keywords

Onychophorans, A. keerensis

An investigation of Onychophora (velvet worms) of the Illawarra region

Christie Chapman

Supervisors: Prof. James Wallman and Dr Mandy Reid

A research report submitted in partial fulfilment of the requirements for the award of the degree of

Bachelor of Environmental Science (Honours)

School of Earth and Environmental Sciences, Faculty of Science, Medicine and Health
The University of Wollongong, New South Wales, Australia

October 2018

DECLARATION

The information in this thesis is entirely the result of investigations conducted by the author, unless otherwise acknowledged, and has not been submitted in part, or otherwise, for any other degree or qualification.

Signed: CHRISTIE CHAPMAN

Date: 23/10/2018

ACKNOWLEDGEMENTS

I would like to acknowledge my supervisors, James Wallman and Mandy Reid, who provided an unlimited amount guidance and feedback throughout my project, which allowed me to develop new scientific skills. Your passion for biology has inspired me to pursue a career in taxonomic research one day. I also need to thank you for giving me the motivation and drive to succeed, and to finish this project with a feeling of pride and accomplishment, rather than exhaustion.

I would also like to acknowledge Andrew King and Ingo Burghardt for your aid in the lab. You taught me the fundamentals of DNA extractions and amplifications, and provided comprehensive assistance with troubleshooting, especially when I had no idea what I was doing. I started this project with minimal knowledge on how DNA is extracted and amplified, but now I can comfortably and independently conduct these procedures with efficiency. Additionally, I need to thank Tracey Gibson for providing excellent troubleshooting assistance and feedback with interpreting gel electrophoresis results.

I also need to thank Blake Dawson and Nathan Butterworth for providing quick and comprehensive feedback whenever it was needed and helping with field work. A special thanks to Nikolas Johnston for teaching and assisting me with detailed phylogenetic analyses, along with simple concepts such as protein translation. You all helped enormously by helping to fix any mistakes before James or Mandy got to see them.

I'd like to thank Jim Lewis for giving me a huge amount of support and spending countless hours flipping over logs and searching through leaf litter with me. I also need to thank others who assisted with field work including Braden Riles, Ian Bool, Thomas Burley, Sabrina Velasco, Cindy Chapman and Chloe Chapman.

I would also like to thank the staff at the Australian Museum Research Institute and Macquarie University for providing a welcoming environment and laboratory facilities and equipment. Thank you to Chao Shen and Sue Lindsay for helping me operate the Scanning Electron Microscope. I also need to thank Fredrica Turco from the Australian National Insect Collection and Graham Milledge at the Australian Museum for the loan of specimens from their collections.

Thank you to Marina McGlinn for always taking great care of your honours students by providing delicious sandwiches and various emails making sure we are progressing and sleeping well.

ABSTRACT

Onychophorans are a fascinating phylum of terrestrial invertebrates that form a group with the Arthropoda and Tardigrada known as Panarthropoda (Campbell *et al*. 2011). Diversity among the Onychophora has been grossly underestimated as their conserved morphology results in the prevalence of cryptic species, whereby two or more species may be grouped under one species name if gross morphology alone has been used as the only means of identification. In recent years, more detailed morphological analyses and the application of molecular analyses has shed more light on diversity among the Onychophora. Within this phylum, two families have been recognised, the Peripatopsidae and Peripatidae, with a lack of any higher taxonomic ranks. The family Peripatopsidae are found in Australia, New Zealand, South Africa, and New Guinea and currently consists of many monotypic genera. One of these, *Anoplokaros*, with its single species *Anoplokaros keerensis* Reid, 1996, was originally suggested to comprise a likely cryptic species-complex (Reid 1996). This hypothesis was tested within this study, employing an integrative taxonomic approach, involving both molecular and morphological analyses. It was revealed that three putative novel species are present within the Illawarra region, that were previously believed to be populations of *A. keerensis*. Unique morphological characters were observed in most of the populations examined, although these were not necessarily congruent with the mtDNA COI sequences. Morphological descriptions were also prepared for additional specimens that were not included in the phylogenetic analyses that could be used as a baseline to facilitate future revisions of these putative *A. keerensis* populations.

TABLE OF CONTENTS

DECLARATION.....ii

ACKNOWLEDGEMENTS iii

ABSTRACT.....iv

LIST OF FIGURES vii

LIST OF TABLES viii

1. INTRODUCTION.....1

2. METHODOLOGY 5

2.1 Material examined.....5

2.2 Molecular analyses 6

2.2.1 Tissue types examined 6

2.2.2 DNA extractions.....7

2.2.3 PCR and Primers 7

2.2.4 Phylogenetic analysis.....8

2.3 Morphological analyses.....10

2.3.1 Morphology: overview 10

2.3.2 Body colour and pattern 11

2.3.3 Microscopy 11

2.3.4 Internal anatomy 11

3. RESULTS 13

3.1 Molecular analyses 13

3.1.1 Tissue types examined 13

3.1.2 Extractions and PCR 13

3.1.3 Phylogenetic analysis.....14

3.2 Morphological Analyses.....16

3.2.1 Body Colour and Pattern.....16

3.2.2 Scanning Electron Microscopy 17

3.2.3 Internal anatomy 28

4. DISCUSSION 33

4.1 Molecular analyses 33

4.1.1 Tissue types 33

4.1.2 Application of COI to delineate species 33

4.1.3 PCR and Sequencing 34

4.1.4 Barcode gap analysis: Is sequence divergence outside intra-specific limits 35

4.1.5 Assessment of Maximum Likelihood Analysis 37

4.1.6 Implications of phylogenetic analyses 37

4.2 Morphological Analyses 38

4.2.1 Application of Morphology 38

4.2.2 Body colour and pattern 39

4.2.3 Scanning Electron Microscopy 39

4.2.4 Internal anatomy 41

4.2.5 Implications of morphology 41

4.3 Integrative taxonomy 42

5. CONCLUSIONS 46

REFERENCES 48

APPENDICES 57

LIST OF FIGURES

Figure 1. Locality map for specimens examined 5
Figure 2. Primary onychophoran morphological features 10
Figure 3. Labelled diagram of dissected male onychophoran 12
Figure 4. Phylogenetic relationships among specimens examined. 15
Figure 5. Simplified diagram of repeated pattern extending from anterior to posterior. 16
Figure 6. Comparison of body pattern for two colour morphs 17
Figure 7. Antennae 18
Figure 8. Anterior accessory gland, character state 1 19
Figure 9. Anterior accessory gland, character state 2 19
Figure 10. Anterior accessory gland, character state 3 20
Figure 11. Anterior accessory gland, character state 4 20
Figure 12. Crural gland on 2nd oncopod pair, character state 1 21
Figure 13. Crural gland on 2nd oncopod pair, character state 2 22
Figure 14. Gonopore, character state 1 23
Figure 15. Gonopore, character state 2 23
Figure 16. Nephridiopore, character state 1 24
Figure 17. Nephridiopore, character state 2 25
Figure 18. Nephridiopore, character state 3 25
Figure 19. Primary papillae, character state 1 26
Figure 20. Primary papillae, character state 2 27
Figure 21. Primary papillae, character state 3 27
Figure 22. Primary papillae, character state 4 28
Figure 23. Male reproductive tracts and associated glands; anterior accessory gland, character state 2 29
Figure 24. Male reproductive tracts and associated glands; anterior accessory gland, character state 2 30
Figure 25. Male reproductive tracts and associated glands; posterior accessory gland, character state 1 31
Figure 26. Phylogenetic relationships among specimens examined 44

LIST OF TABLES

Table 1. Sample accession numbers and collection locations.....6
Table 2. Primer names, sequences and positions 7
Table 3. Functions attributable to structures labelled in Figure 2 11
Table 4. Number of specimens (N) with molecular data available from each site 14
Table 5. K2P distances.....14

1. INTRODUCTION

Onychophorans, commonly known as velvet worms, are terrestrial soft-bodied invertebrates, possessing 13 to 43 leg pairs, referred as oncopods (Mayer *et al.* 2015). These animals inhabit moist microhabitats created by decomposing wood and leaf litter where they prey on other small invertebrates such as termites, crickets, cockroaches, centipedes, spiders, worms, and even large snails (Read & Hughes 1987; Dias & Lo-Man-Hung 2009). Velvet worms employ a hunting and defence mechanism unique among terrestrial invertebrates, which involves the ejection of an adhesive slime secretion from modified oncopods located next to their mouth (Baer & Mayer 2012). This secretion is protein-based and allows velvet worms to nocturnally catch their prey and then feed upon them by firstly injecting them with salvia to immobilise them, which may also start to break down the flesh (Mayer *et al*. 2015). The slime-covered prey is then slowly ingested along with their slime (Haritos *et al*. 2010). The Onychophora are of great interest taxonomically as this phylum is considered the sister clade to Arthropoda (insects, arachnids, myriapods, and crustaceans) which, along with Tardigrada (water bears), form a taxon known as Panarthropoda (Campbell *et al*. 2011). This makes onychophoran taxonomic studies important as they may provide information that assist in research on Panarthropodal origins as little is known about the morphology of ancestral panarthropods (Ou *et al*. 2012). This information may also help shed more light on the evolutionary complexity and diversity among extant panarthropods (Budd & Telford 2009).

The Onychophora are divided into two families, the Peripatidae and Peripatopsidae, with a lack of higher taxonomic ranks. Peripatids are primarily found in Central America, northern South America, and southeast Asia, whereas peripatopsids are found in Australia, New Zealand, South Africa, and New Guinea (Oliveria *et al.* 2011). Conversely, Australia is home to the majority of the world's known peripatopsid species, with 80 described species and possibly many more that remain undescribed (Reid 1996, 2000, 2002; Rockman *et al.* 2001; Ruhberg & Daniels 2013). Peripatopsidae are a diverse family, and employ a range of reproductive strategies, including several different methods of insemination, specialised secondary sexual structures and several embryonic nourishment modes (Mayer *et al.* 2015). These specialised secondary sexual structures can be of great taxonomic importance, and include a unique range of head modifications, such as pits, spikes, modified papillae and eversible structures found in males (Tait & Briscoe 1990). These head structures function in a wide range of complex mating behaviours, which include dermal spermatophore transfer and possibly female attraction and mate choice (Tait & Norman 2001; Reinhard & Rowell 2005). Onychophorans also have surprisingly large and well-developed brains, with neuroanatomical

studies suggesting that their behaviour may be even more complex than previously documented (Strausfeld *et al*. 1998). For example, it has been observed in a peripatopsid species, *Euperipatoides rowelli* Reid 1996, that female-dominant social groups are formed, that hunt collectively and have hierarchies established by aggressive-dominant and passive-subordinate individuals (Reinhard & Rowell 2005).

Onychophoran's have a conserved morphology that appears to have changed relatively little since the Cambrian (Liu *et al.* 2008). This contrasts with other invertebrate phyla such as the Arthropoda that possess countless morphological forms. Their lack of segmentation and tagmosis (the evolutionary process that leads to modification of segments) may be a reason for the lack of morphological variation within the phylum. Furthermore, their invariant body structure may be due to diversification in other forms, such as chemical or behavioural modifications. Pheromones, for example, play a key role in onychophoran communication (Reinhard & Rowell 2005) and may be useful for discriminating cryptic species, as suggested by Bickford *et al.* (2007). Perhaps their morphological form is so extremely efficient for surviving within saproxylic environments, the need to modify morphologically has been eliminated. This morphological conservatism results in a limited number of variable characters being available for use in taxonomy that creates difficulty when diagnosing and documenting species boundaries. In many cases, this can create a challenge as cryptic species-complexes are often a resultant of this misidentification (Oliveira *et al*. 2011; Ruhberg & Daniels 2013).

Onychophorans are saproxylic and are restricted to the moist microhabitats within decomposing wood and leaf litter as they lack any advanced desiccation-resistant structures (Barclay *et al.* 2000). Their morphology is unfavourable to wide-range dispersal as rapid water loss in dry conditions can be fatal. Limited mobility can result in strong complex local endemism and create high genetic intraspecific diversity as seen in *E. rowelli*, found in south-east New South Wales, Australia (Bull *et al.* 2013). This high genetic diversity could also be a product of the role geography plays on spatial genetic structuring, as a history of peri-glaciation on the east coast of Australia would have led to repeated habitat reorganisation. When a habitat is reorganised by a powerful natural force, it is likely that refugees are able to become re-established when conditions change, and viable habitat is restored. When this process occurs, reorganisation of genetic structure may also be permitted, resulting in an increase of genetic variance (Porter 1999). To support these contentions, a molecular study conducted among members of the speciose genus, *Planipapillus* Reid 1996, located throughout the alpine region of eastern Australia, revealed less mtCOI sequence divergence than a population of *E. rowelli* found in a single log (Gleeson *et al*. 1998; Rockman *et al*. 2001). This is most likely due to the

fact that the alpine regions of Australia were once glaciated therefore eradicating, rather than reorganising, entire habitats with little opportunity for refugees to recolonise in suitable remnant habitats.

Onychophorans exhibit one of the most extreme forms of short-range endemism within the animal kingdom (Harvey 2002). Their dependence on specific microhabitats confines them to discontinuous habitats with little dispersal potential. Human-induced changes can therefore have significant influences on habitat suitability and subsequent species survival. Conservation of 'hot-spots' would ensure the preservation of the maximum number of taxa exhibiting short-range endemism. This would also allow the conservation of underlying ecological processes that assisted the formation of these species. Short-range endemic species could also be an indicator of specific habitat conditions able to support biodiversity beyond what is currently known. Invertebrates in particular have the reputation for being neglected in biodiversity conservation policies due to several impediments, such as lack of research and knowledge, as well as discreet charismatic value (Cardoso *et al.* 2011).

The ambiguity in the taxonomy of invertebrates such as onychophorans results in the need for a combination of morphological and molecular analyses as a holistic taxonomic tool to fully understand these groups. Multidisciplinary taxonomic approaches have the potential to overcome the challenges arising from the sole use of morphology, as this can be highly problematic (Daniels *et al*. 2009). Cain (2014) suggests that traditional taxonomic practices that rely only on a single discipline should not be used to understand biodiversity. Taxonomic studies that involve both morphological and molecular analyses therefore have the potential to produce more robust species delineations. This approach is known as 'integrative taxonomy' and can be defined as the science that aims to delimit the units of biodiversity from multiple and complementary perspectives (Dayrat 2005). Integrative approaches are extremely important as the complexity of life requires that species boundaries are studied from multiple perspectives, especially when dealing with groups, such as velvet worms, where morphological features may be relatively limited. Clearly, multidisciplinary tools should be employed while attempting to undergo taxonomic studies on the Onychophora in order to obtain a comprehensive understanding of species boundaries.

A revision of Australian peripatopsid species by Reid (1996) revealed many monotypic genera. An example is *Anoplokaros* Reid 1996, with its single species, *Anoplokaros keerensis* Reid 1996. This putative species has a broad distribution within the Illawarra region in New South Wales, Australia, ranging from the Royal National Park to Cambewarra Mountain covering over 2000 km^2, which is unusually large among other species studied in detail to date

(Ruhberg & Daniels 2013). *Anoplokaros keerensis* has also had several specimens tentatively assigned to it which were said to differ from the type specimens found on Mount Keira, New South Wales, Australia, with some variability in morphological features (Reid 1996). Reid (1996: page 733) noted, 'The presence of a cryptic species-complex is suspected by considerable electrophoretic differences found between specimens probably referable to the taxa listed here. Detailed examination of additional characters (e.g. molecular characters) followed by reassessment of morphological features, is needed to resolve species boundaries over the range of this putative complex.' As previously mentioned, morphological ambiguity and previous documentation of high levels of local endemism in onchophorans suggests that many widespread taxa may actually comprise more than a single species that need to be taxonomically revised using an integrative taxonomic approach.

This study presents an examination of the populations tentatively assigned to *Anoplokaros keerensis* from a number of locations across its supposed distributional range. This will be undertaken using both morphological and molecular techniques to determine whether this taxon as currently defined represents one or more, perhaps cryptic, species. This study aims to utilise these integrative techniques to delineate this putative cryptic species-complex.

2. METHODOLOGY

2.1 Material examined

Collection sites were selected based on museum and published records of locations where the putative *A. keerensis* had been collected in the past within the Illawarra region (Table 1). However, of these sites, specimens were only collected from Mount Keira, Austinmer and Mount Gibraltar Nature Reserve between February and June 2018. These were found inside and underneath rotting logs at varying stages of decomposition, as well as on the undersides of rocks in forested areas on the south east coast of Australia (Fig. 1). Various collection methods were employed such as manual searches through leaf litter and pitfall traps, although only manual searches resulted in specimen collection. Collected onychophorans were stored in small plastic containers with a piece of moist wood or soil until they were anaesthetised with ethyl acetate and preserved in 95% ethanol. Specimens were photographed with a Nikon DSLR D3100 (Nikon, Sydney, NSW, Australia) and used in both molecular and morphological analyses.

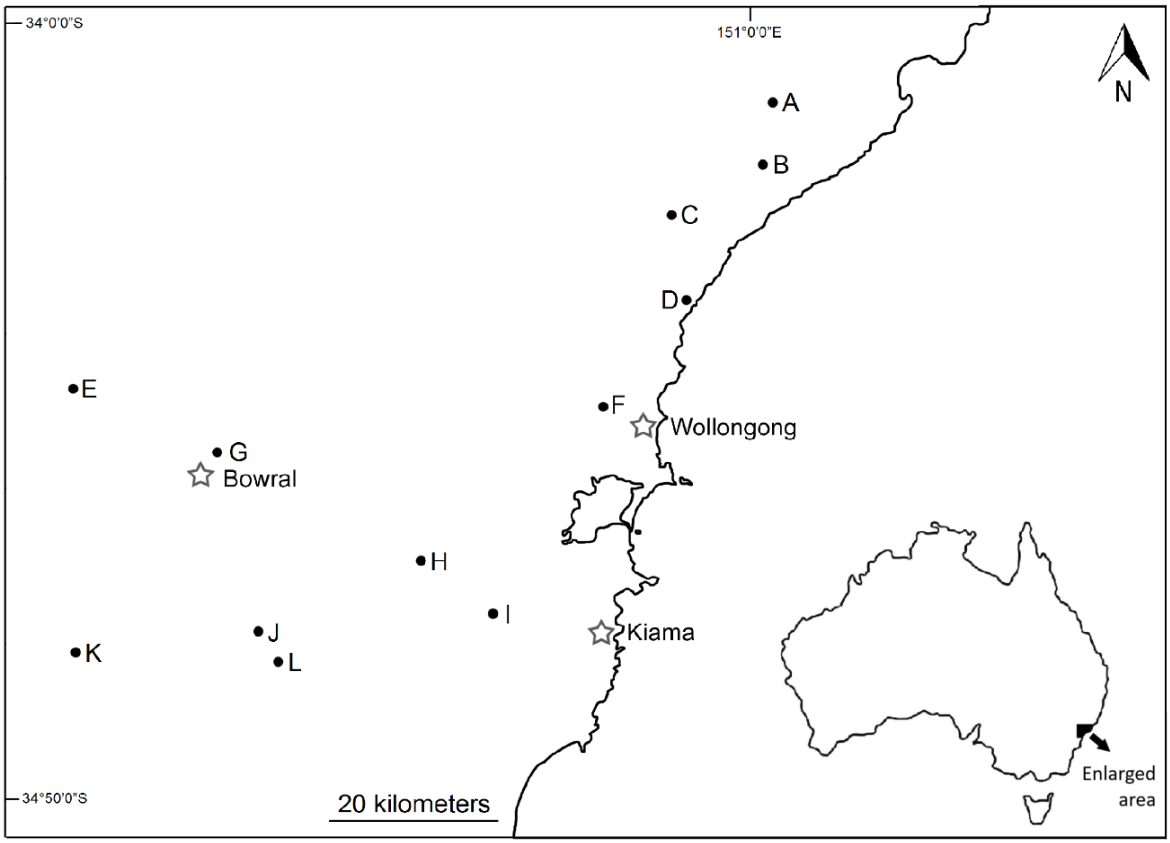

Figure 1. Locality map for specimens examined. Uppercase letters at each black dot indicate the following localities: (A) Heathcote, (B) Royal National Park, (C) Darkes Forest, (D) Austinmer*, (E) Twin Falls, (F) Mount Keira*, (G) Mount Gibraltar Nature Reserve*, (H) Macquarie Pass National Park, (I) Budderoo National Park, (J) Avoca, (K) Bundanoon, (L) Barrengarry Mountain. *Indicates sites where specimens were collected during this study (See Table 1 for more details).

Specimens were borrowed from the Australian Museum and the Australian National Insect Collection to include in the integrative analyses. Some of these preserved museum specimens were appropriate to use for molecular analyses, although others had been fixed in formalin (formaldehyde) and thus not suitable for DNA extractions (Do & Dobrovic 2015). These specimens were therefore were only viable for morphological assessment.

The available material was limited and, in some cases, only one specimen was available for examination per site. For example, the single museum specimen from the Royal National Park was female, therefore reducing the number of viable comparative characters to include in the morphological analysis, as some characters examined are male-specific (Table 1).

Table 1. Sample accession numbers and collection locations.

Accession no.	N	Locality	Coordinates
AM.CC1	1	Heathcote	34°05’5.2” S, 151°01’28.8” E
AM.CC2	1	Royal National Park	34°09’6.9” S, 151°00’51.4” E
AM KS.91348*	4	Darkes Forest	34°12’0.0” S, 150°55’0.0” E
AM.CC3	1	Austinmer	34°17’51.0” S, 150°55’55” E
AM KS.28191	4	Twin Falls	34°23’42.0” S, 150°16’48.0” E
ANIC 852	1	Twin Falls	34°23’23.9” S, 150°16’48.0” E
AM.CC4*	3	Mount Keira Scout Camp	34°24’4.0” S, 150°50’39.1” E
AM.CC5*	5	Mount Gibraltar Nature Reserve	34°28’0.8” S 150°25’50.4” E
AM KS.045948	2	Macquarie Pass National Park	34°34’0.0” S, 150°39’0.0” E
AM KS.119248*	2	Budderoo National Park	34°38’02” S, 150°43’37” E
AM KS.28199	5	Avoca	34°37'0.0" S, 150°29'1.0" E
AM KS.16580	5	Bundanoon	34°40’31.5” S, 150°16’51.9” E
AM KS.119221*	2	Barrengarry Mountain	34°41’08.0” S, 150°29’52.0” E
ANIC 48	3	Barrengarry Mountain	34°41’08.0” S, 150°29’52.0” E

N, number of samples examined
*, indicates molecular analyses were conducted on specimens
AM KS, Australian Museum collection registration numbers
ANIC, Australian National Insect Collection registration numbers

2.2 Molecular analyses

2.2.1 Tissue types examined

Several tissue types were initially used from six specimens from Mount Keira, Mount Gibraltar, Austinmer and Darkes Forest to determine the most effective tissue type to use for DNA extractions. This preliminary study was also undertaken to determine which tissue can provide the cleanest sequence, as Sunnucks and Wilson (1999) mentioned dermal pigments can act as PCR inhibitors. These tissues include muscle tissue (located on the internal body wall),

lateral nerve cord, pigmented embryos and ovaries, mouth tissue, and small sections of pigmented dermal tissue attached to muscle tissue.

2.2.2 DNA extractions

Genomic DNA was extracted from tissues (about 25 mg) using ISOLATE II Genomic DNA Kit (Bioline, London, UK) according to the manufacturer's protocol.

2.2.3 PCR and Primers

Amplification of the 659 bp (1816–2518 bp) barcode region of COI (*cytochrome c oxidase subunit I*) was performed using the primer combination LCO1490 and HCO2198 (Folmer *et al.* 1994, Table 2). Individual PCR reactions contained: 5 µl MyTaq Red Reagent Buffer (Bioline, London, UK), 0.2 µl MyTaq Red DNA Polymerase (Bioline, London, UK) and 2 µL of genomic DNA. Cycling conditions were: 1 cycle of 94°C for 2 min; 38 cycles of 94°C for 30 s, 50°C for 45 s, and 72°C for 1 min; 1 cycle of 72°C for 3 minutes.

Two other fragments of COI were also amplified (1816–2668 bp and 2511–2938 bp) using the primer combinations of LCO1490/HCOoutout and HCOextA/HCOextB respectively, to obtain a continuous >1000 bp sequence, once concatenated (Prendini *et al*. 2005, Table 2). These will be referred to as 'fragment 2' and 'fragment 3', respectively. Cycling conditions for these fragments were: 1 cycle of 94°C for min; 38 cycles of 94°C for 30 s, 46°C for 40 s, and 72°C for 40 s; 1 cycle of 72°C for 5 min. Difficulties arose when attempting to amplify 'fragment 2' with the reverse primer HCOoutout and this was subsequently replaced by HCO2198 amplifying a slightly shorter fragment (barcode region, 1816—2518 bp).

Table 2. Primer names, sequences and positions

Primer Name	Primer Sequence	Position
LCO1490	5' – GGT CAA CAA ATC ATA AAG ATA TTG G – 3'	1816–1834
HCO2198^{+}	5'– TAA ACT TCA GGG TGA CCA AAA AAT CA – 3'	2518–2493
HCOoutout^{+}	5' – GTA AAT ATA TGR TGD GCT C – 3'	2536–2511
HCOextA	5' – GAA GTT TAT ATT TTA ATT TTA CCT GG – 3'	2511–2536
HCOextB^{+}	5' – CCT ATT GAW ARA ACA TAR TGA AAA TG – 3'	2938–2913

$^{+}$ indicates reverse primer

Electrophoresis was undertaken to determine whether each PCR amplification was successful. This was done by loading 3 µl of the PCR product into each well of the agarose gel.

In gel stain GelRed® (Biotium, California, USA) was used to visualise the presence and size of DNA fragments after running 70 V through the gel for 50 min. PCR amplicons were visualised by Gel Doc™ XR+ Gel Documentation System (Bio-Rad, Gladesville, NSW, Australia).

Prior to sequencing amplicons were purified using ExoSAP-IT™ PCR Product Clean-up Reagent (Thermo Fisher Scientific, Massachusetts, USA) using 25 µl of the PCR product and 1.5 µl of Exo-SAP-IT. This mixture was then incubated at 37°C for 15 min before the ExoSAP was inactivated at 80°C for 15 min with a final step at 10°C for 5 min. This process allows clean-up of the PCR product without sample loss as it is not subject to precipitation or column separation (Dugan *et al.* 2002). Purified PCR products (referred to as a template) and sequencing primer were pre-mixed and loaded onto a plate. For each sample, 10 µl of template and 1 µl of primer were loaded into a well position for both the forward and reverse primers. The plates were submitted for Sanger Sequencing by the Australian Genome Research Facility (AGRF, Melbourne, Victoria, Australia). This facility uses an Applied Biosystems™ 3730 DNA Analyser (Thermo Fisher Scientific Massachusetts, USA). Cycling conditions for sequence reactions were: 1 cycle of 96°C for 2 min; 30 cycles of 96°C for 10 s, 50°C for 5 s, and 60°C for 4 min; then hold at 4°C.

2.2.4 Phylogenetic analysis

Sequence electropherograms for all amplified COI sequences were edited using ChromasPro 1.33 (Technelysium Pty Ltd, Tewantin, QLD, Australia; available from: www.technelysium.com.au/ChromasPro.html). As such, the 659 bp 'barcode' region and the 427 bp fragments ('fragment 3') were concatenated into a single sequence. The contiguous chromatograms were concatenated and edited using ChromasPro and then aligned using the Clustal W algorithm (Thompson *et al.* 1994) with the default parameters, i.e., gap opening penalty (GOP) = 15.00, gap extension penalty (GEP) = 6.66, transition weight = 0.50 and delay divergent cut-off = 30%. This was executed in MEGA (MEGA X 10.0.1: Molecular Evolutionary Genetic Analysis, Kumar *et al.* 2016). An additional sequence for the onychophoran *Ooperipatellus cryptus* Jackson & Taylor, 1994 was obtained from GenBank (accession number: KC754662, www.ncbi.nlm.nih.gov/genbank) and added to the alignment to serve as an outgroup. The reliability of *O. cryptus* as an outgroup was initially tested using an alternate outgroup from the Peripatidae, *Peripatus dominicae* Pollard, 1893 (Appendix 1–

3). *Ooperipatellus cryptus* did not cluster within the peripatopsid taxa included in this study and was thus used as an outgroup.

Aligned sequences were then submitted to the online Automatic Barcode Gap Discovery tool (ABGD; Puillandre *et al*. 2012). This calculated pairwise genetic distances using Kimura's two-parameter model (K2P, Kimura 1980) and sorted the COI barcoding region sequences into hypothetical species based on the 'barcode gap'. This 'gap' is created by pairwise differences whenever the divergence among organisms belonging to the same species is smaller than divergence among organisms from different species. This was executed without the inclusion of the outgroup.

Following barcode gap analysis, aligned, concatenated sequences were submitted for analysis by RAxML-HPC v. 8 (Stamatakis 2014) on the online platform CIPRES Science Gateway (Miller *et al.* 2010, Available from: http://www.phylo.org/). The dataset was split into three partitions based on the first, second and third codon positions. These partitions were then submitted to PartitionFinder v.2 (Canberra, ACT, Australia) to select the optimal model for each partition. The model GTR with Gamma distribution was chosen, and Maximum Likelihood (ML) analysis was performed using 500 bootstrap iterations. The resultant trees were then visualised and edited in Fig-Tree v.1.4.3 (Institute of Evolutionary Biology, University of Edinburgh, Scotland, Available from: http://tree.bio.ed.ac.uk/).

This analysis procedure was replicated for four different sequences alignment configurations, to ensure accuracy of the final phylogenetic hypothesis: 1) only the 'barcode' region sequences (Appendix 1), 2) only 'fragment 3' sequences (Appendix 2), 3) only the sequences where the 'barcode' region and 'fragment 3' were concatenated (Appendix 3) and 4) all sequences concatenated (Fig. 4). It was determined by comparison of all resultant ML trees that including specimens for which both COI fragments were unavailable had no obvious effect on the observed phylogenetic results. It was therefore decided to use the alignment configuration containing all sequences available regardless of size or location.

2.3 Morphological analyses

2.3.1 Morphology: overview

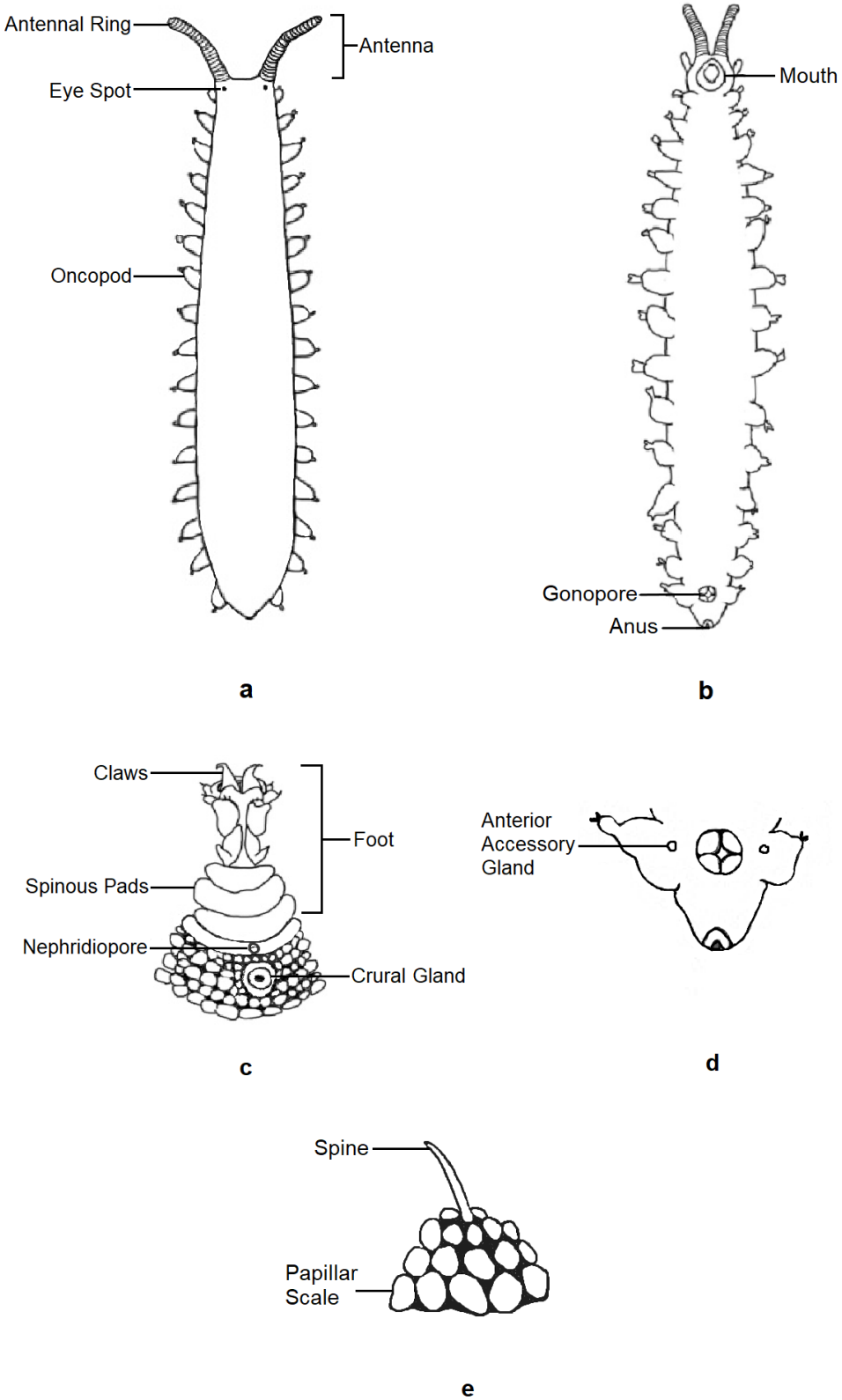

Figure 2. Primary onychophoran morphological features: (a) entire animal, dorsal view; (b) entire animal, ventral view; (c) distal oncopod and foot, ventral view; (d) posterior end of body, ventral view; (e) distal tip of a primary papilla.

Table 3. Functions attributable to structures labelled in Figure 2.

Structure	Function
Antennae	Sensory perception.
Antennal Rings	Usually 30. Covered in mechanoreceptive spines.
Anterior Accessory Gland	Only present in males. Function unknown but assumed to secrete pheromones.
Crural Gland	Only present in males. Secrete pheromones.
Gonopore (or Genital Pad)	Opening to genital tract in both sexes.
Nephridiopore	Waste excretory organ. Only present ventrally on the 4th and 5th oncopod pair.
Papillae	Cover entire body. Protrusions known as 'papilla bristles' or 'spines' may have mechanoreceptive abilities.

2.3.2 Body colour and pattern

Light photomicrography was used to compare colour and body pattern of the dorsal dermal integument. The pattern and pigmentation have been said to differ in *A. keerensis* specimens between sites (Reid 1996).

2.3.3 Microscopy

Tissue samples dissected from 22 preserved specimens collected from various locations were dissected, then individually mounted on specimen stubs on adhesive carbon disks to air dry as a time-saving and inexpensive alternative to critical-point drying, which would have required more handling or possibly tissue damage (Bray *et al.* 1993). The specimen stubs were then gold coated in an EMITECH K550 Gold Sputter Coater and studied using a JSM-7100F (JEOL LTD.) Field Emission Scanning Electron Microscope (SEM). For each male specimen, the antennal rings, anterior accessory gland, crural gland, genital opening (gonopore), nephridiopore and papillae were examined (Fig. 2, Table 3). In females, only the antennal rings, genital opening (gonopore), nephridiopore and papillae were examined. The width between eyespots (referred to as 'HWE') was measured for each specimen included in the morphological analyses as a standardised measure of size, following Reid (1996). The primary papillae character states were plotted against the molecular results as an integrative approach to differentiating the populations examined as this character appeared to be the most diagnostic.

2.3.4 Internal anatomy

The internal anatomy was examined following dissection. A longitudinal incision along the mid-dorsal line from the anal opening, extending anteriorly for two-thirds of the body length. Two transverse cuts were then made at the anterior end of this incision, making it

possible to pull back and pin the body wall to a wax plate to reveal internal structures. Males were dissected to examine the reproductive tracts and associated glands as these characters have been used as diagnostic characters in other peripatopsids (Reid 1996). Females were also dissected to determine the presence or absence of embryos in that later stages of development, as *A. keerensis* was said to be ovoviviparous (Reid 1996). These results are presented within the morphological descriptions of each population (Appendix).

Animals were dissected under the relevant storage solution, either 70% or 95% ethanol and examined under a Leica MZ16A microscope (Leica Microsystems) and photographed with a Leica DC digital camera. The shape and size of reproductive organs and associated glands such as the anterior accessory gland, posterior accessory gland, testes, seminal vesicle, vas deferens and vas efferens were photographed and traced in Adobe Photoshop (Adobe) to produce clear outlines of each structure.

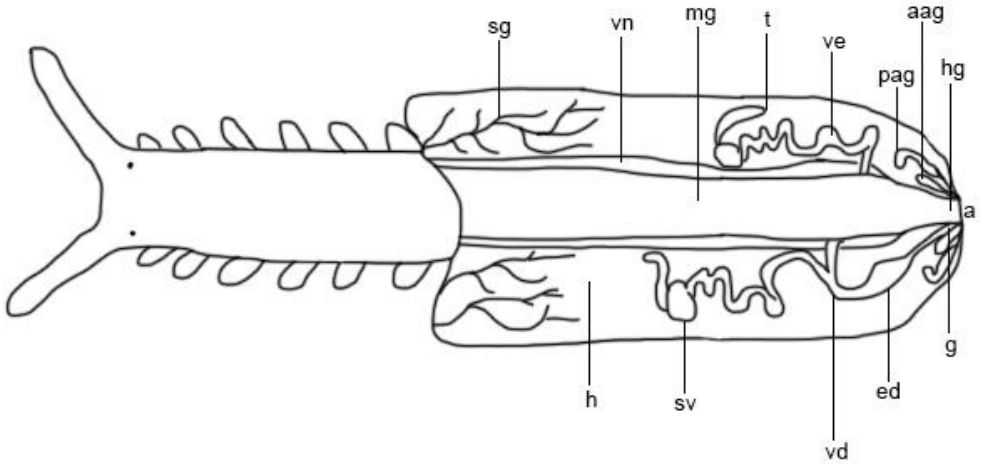

Figure 3. Labelled diagram of dissected male onychophoran. Abbreviations; sg, slime gland; vn, ventral nerve cord; mg, midgut; t, testis; ve, vas efferens; hg, hindgut; a, anus; g, gonopore; ed, ejaculatory duct; vd, vas deferens; sv, seminal vesicle; h, hemocoel.

3. RESULTS

3.1 Molecular analyses

3.1.1 Tissue types examined

The tissue type used for DNA extractions did not influence the quality of the sequence data obtained for six specimens collected from Mount Keira, Mount Gibraltar, Austinmer and Darkes Forest. These tissue types included muscle tissue (located on the internal body wall), lateral nerve cord, embryos and ovaries, mouth tissue, and small sections of pigmented dermal tissue attached to muscle tissue. This preliminary study enabled plasticity when further extractions took place, as it had already been determined that successful sequences were not reliant on specific tissue types. It was also determined that the presence of pigments in the dermal integument and embryos did not inhibit the PCR, as was observed by Sunnucks and Wilson (1999).

3.1.2 Extractions and PCR

In total, 14 specimens were selected to be included in molecular analyses from a range of locations in the Illawarra region, New South Wales within the previously documented distribution of supposed *Anoplokaros keerensis*. Of these specimens, DNA extractions were obtained from 11 specimens. The three specimens from which DNA could not be extracted (one from Heathcote and two from Darkes Forest) were collected up to 20 years ago.

Originally, it was decided to use two fragments of COI, previously referred to as ‘fragment 2’ (amplified with HCOoutout/LCO1490, 1816–2668 bp) and ‘fragment 3’ (amplified with ExtA/ExtB, 2511–2938 bp) to obtain a continuous 1120 bp concatenated sequence. Amplification of ‘fragment 2’ was unsuccessful, so the ‘barcode’ region (amplified with LCO1490/HCO2198, 1816–2518 bp) was chosen as replacement. This decision was made as the ‘barcode’ region had proved to easily amplify onychophoran DNA in the preliminary tissue comparison conducted within this study. The concatenation of the ‘barcode’ and ‘fragment 3’ produced a >1000 bp fragment, although resulted in a 43 bp gap between fragments. Amplification and sequencing of the ‘barcode’ region and ‘fragment 3’ were successful for most extractions. For three specimens, only one of the two fragments could be amplified and sequenced (Table 4). However, based on comparison of all the resultant ML trees, this did not affect the overall result.

Table 4. Number of specimens (N) with molecular data available from each site, with relevant fragments used.

Locality of Collection	N	COI 'Barcode' Region	COI Fragment 3
Mount Keira	3	Yes	Yes
Austinmer	1	Yes	Yes
Barrengarry Mountain	2	No	Yes
Budderoo National Park	1	Yes	Yes
Darkes Forest	1	Yes	No
Mount Gibraltar	3	Yes	Yes

3.1.3 Phylogenetic analysis

The 'barcode' gap and ML analyses revealed consistent and congruent groupings and did not conflict with one another. As single-gene trees were produced using ML analyses, the supported clades were tested using barcode gap analyses as a quantitative approach. The inclusion of the non-barcoding region sequences (fragment 3) in the ML analyses had no effect on the overall tree topology or support for each clade.

It should be noted that the type locality of *Anoplokaros keerensis*, Mount Keira, appeared to be home to two genetically distinct populations. These have been denoted Mt Keira (i) and Mt Keira (ii) in the ML tree below (Fig. 4). The average sequence divergence (obtained from the barcode gap analysis) for Mt Keira (ii) from all other populations was 12% (Table 5).

Table 5. K2P divergences shown as percentages. Mount Keira specimens were grouped based on visual separation in a ML phylogenetic tree.

	Mt Keira (ii)	Budderoo NP	Darkes Forest	Mt Keira (i)	Austinmer	Mt Gibraltar
Mt Keira (ii)	0.00%					
Budderoo NP	12.79%	0.00%				
Darkes Forest	11.50%	2.45%	0.00%			
Mt Keira (i)	12.39%	3.87%	3.03%	0.00%		
Austinmer	12.03%	4.35%	2.41%	1.80%	0.00%	
Mt Gibraltar	12.26%	0.91%	1.96%	3.98%	4.45%	0.00%

Mt, Mount
NP, National Park

Across all populations examined, two main clades were observed: 1) Mount Keira (i) and Austinmer specimens (denoted 'northern' clade in Fig. 4) and 2) Barrengarry Mountain,

Budderoo National Park and Mount Gibraltar specimens (denoted 'southern' clade in Fig. 4). The Darkes Forest specimen separated from both the 'northern' and 'southern' clades in the ML tree, with a mean divergence of 2.5% from the northern and southern populations (bootstrap value = 87, Fig. 4). Mount Keira (ii) separated from all other populations (12%).

Within the 'northern clade', Mt Keira (i) specimens and the Austinmer specimen have a divergence of 1.8%, separating from the Darkes Forest specimen and the 'southern clade' supported by a bootstrap value of 75. Within the 'southern clade', the Barrengarry Mountain population is distinct from the Budderoo National Park and Mount Gibraltar specimens with a bootstrap value of 99 (a sequence divergence value could not be calculated as the 'barcode' region could not be obtained for the Barrengarry Mountain specimens, Table 4). The mean divergence between the Mount Gibraltar and Budderoo National Park specimens is 0.9%.

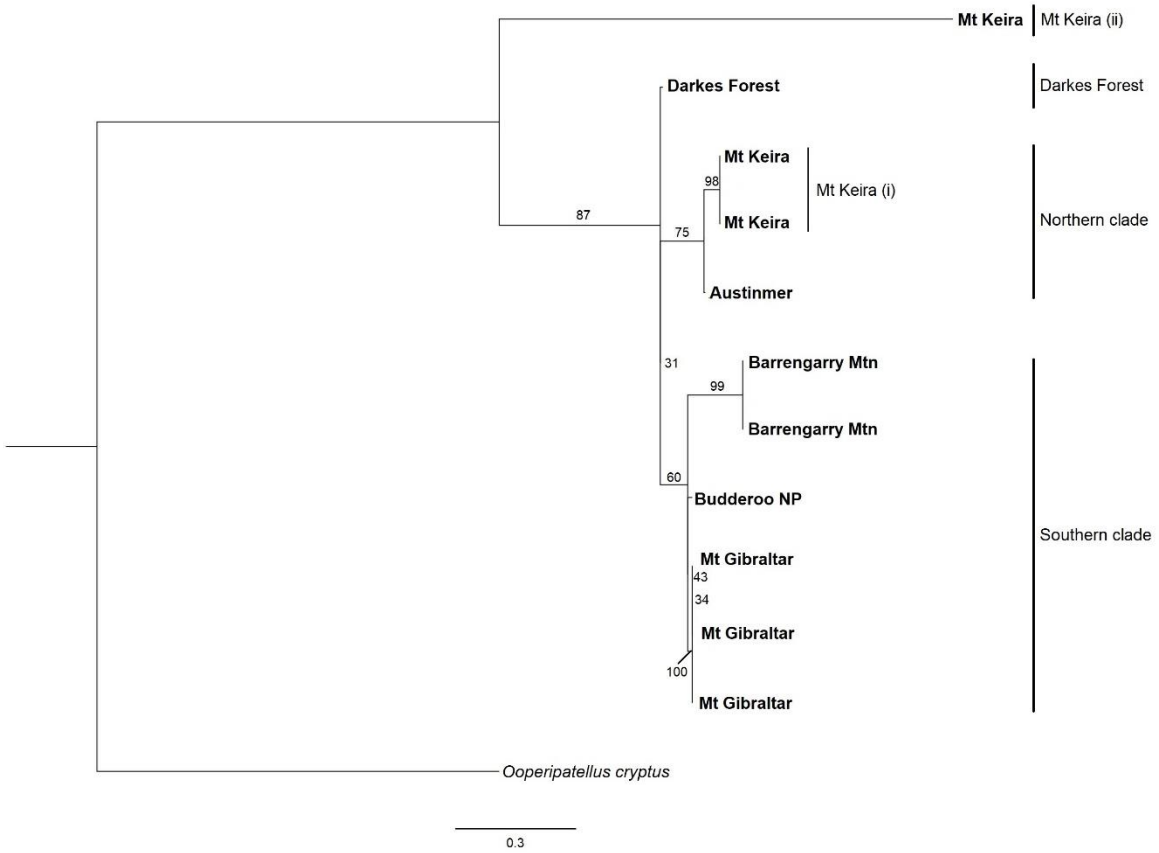

Figure 4. Phylogenetic relationships among specimens examined, including the outgroup taxon, *O. cryptus.* Maximum Likelihood tree constructed from COI nucleotide sequences. Node labels indicate bootstrap support. Bootstrap iterations = 500.

3.2 Morphological Analyses

3.2.1 Body Colour and Pattern

All specimens included in this study possessed the same repeated pattern body pattern that extends from anterior to posterior. The overall pattern has base pigments of brown or blueish tones, with tan and brown or dark grey and black mottles. A dark mid-dorsal stripe extends from anterior to posterior. Short, dark, blotches are present dorsally at every oncopod pair with light patches extending transversely from these dark. Light patches are slightly convex to straight anteriorly and broad U-shaped posteriorly. White papillae are sometimes present on lateral margins of each light transverse patch. This pattern was observed in both sexes (Fig. 5).

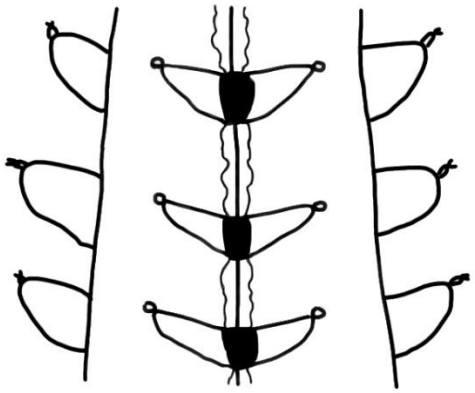

Figure 5. Simplified diagram of repeated pattern extending from anterior to posterior.

Variations in dermal pigmentation was observed in specimens found within and between localities. It appeared that two distinct colour combinations were present, consisting of a combination of browns and blacks, or blues and blacks. The two colour morphs, browns and blacks, and blues and blacks, influenced the distinctiveness of the underlying body pattern. In most cases, the blue-black specimens did not have a clear dermal pattern, while the pattern was clearly visible in brown-black specimens (Fig. 6).

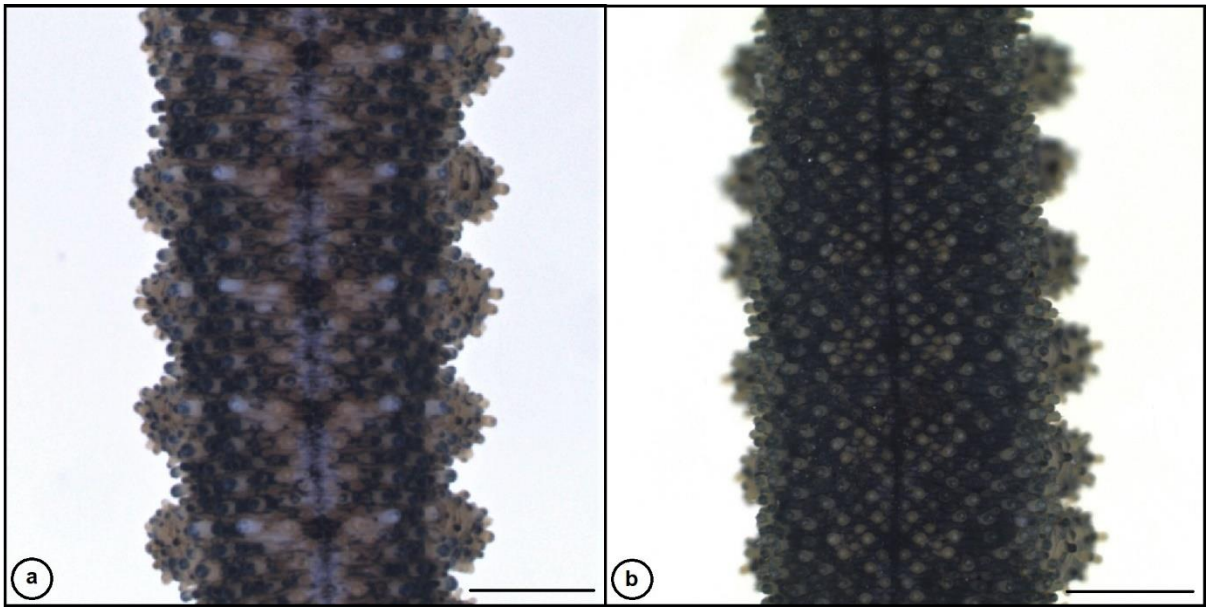

Figure 6. Comparison of body pattern for two colour morphs. (a) Brown-Black colour morph, Barrengarry Mountain, KS.119221, male, 1 mm HWE, scale 0.5 mm; (b) Blue-Black colour morph, Darkes Forest, KS.91348, male, 1.1 mm HWE, scale 0.5 mm.

3.2.2 Scanning Electron Microscopy

Notable morphological variation was observed within this supposed species-complex. Below is a detailed investigation of external characters examined using SEM, as well as descriptions of character states. Overall, the morphological characters provided fewer diagnostic capabilities than expected. For example, the antennal rings were invariant and only two character states were observed in the gonopores.

Antennal Rings

All examined populations was observed to have 30 antennal rings, each with a single row of bristles (Fig. 7a, b).

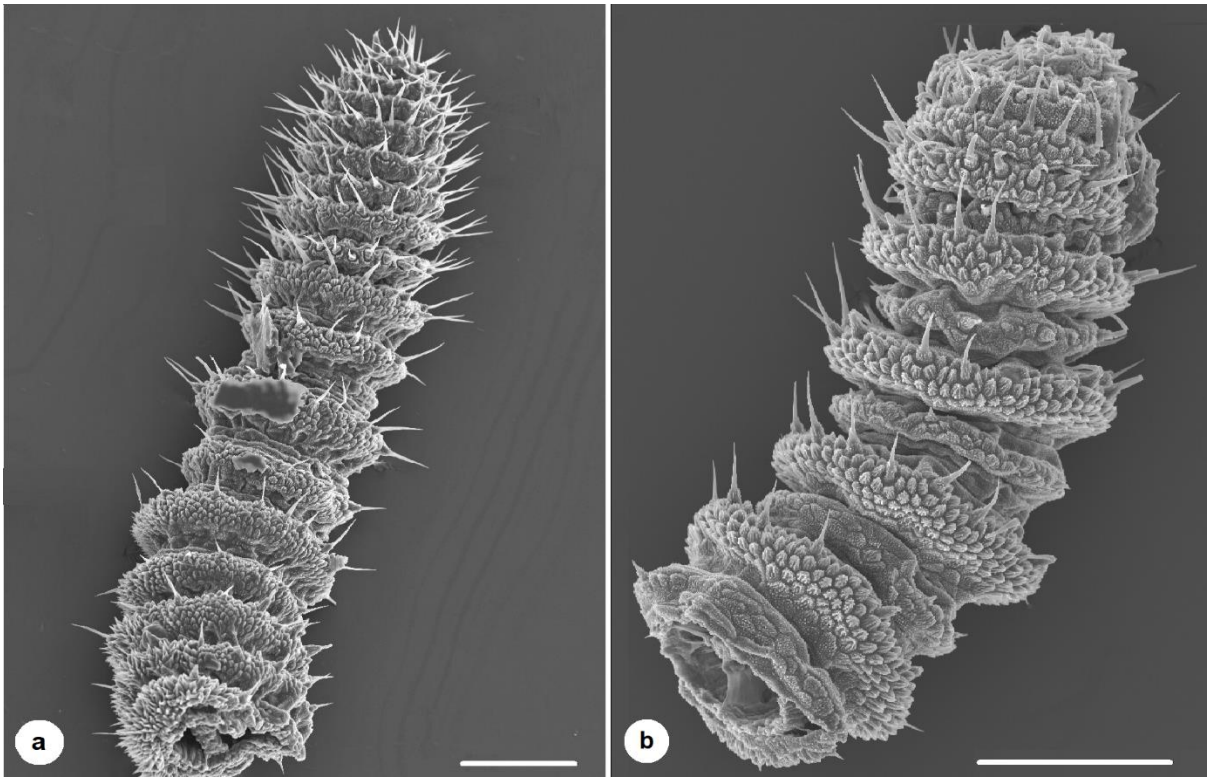

Figure 7. Antennae. (a) Mount Keira (i), AM.CC4, fresh-collected male, 1.2 mm HWE, scale 100 µm; (b) Barrengary Mountain, AM KS.119221, male, 1.1 HWE, scale 100 µm.

This character was observed to be invariant among *A. keerensis* populations. Although the density and number of spines on the antenna appears to be greater in Figure 7a, this was only observed in one specimen. This should be examined further in additional specimens.

Anterior Accessory Glands

These glands are paired structures opening on the ventral side of the last pair of oncopods of males, assumed to secrete pheromones (Reid 1996). Within the populations examined, variations were observed in the structure of the gland opening. The following four character states were recognised:

1, Ribbed papillar scales basally with smooth, broad, lip-shaped distal opening (Bundanoon, Mount Gibraltar, Darkes Forest, Mount Keira (i), Mount Keira (ii), Avoca, and Twin Falls; Fig. 8a, b).

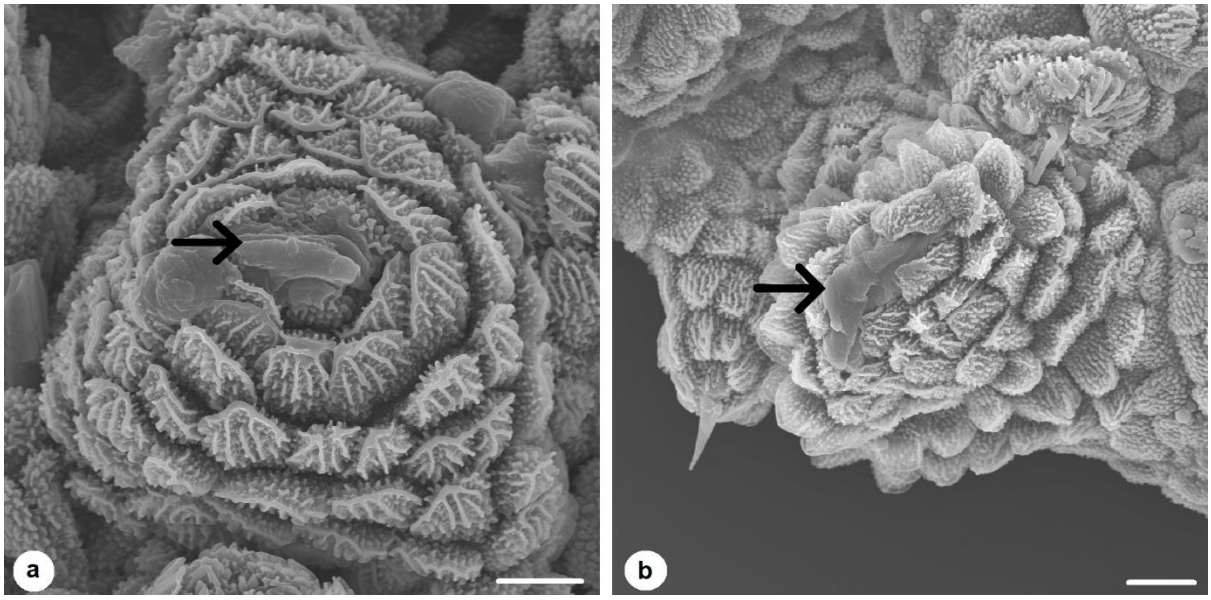

Figure 8. Anterior accessory gland, character state 1. (a) Mount Gibraltar, AM.CC5, fresh-collected male, 1.1 mm HWE, scale 10 µm; (b) Mount Keira, AM.CC4, fresh-collected male, 1 mm HWE, scale 10 µm. Arrows indicate distal openings. (Note: both specimens appear to have some gland exudate attached to the openings.)

2, Ribbed, partially fused papillar scales basaly; smooth, narrow, distal opening (Heathcote; Fig. 9a, b).

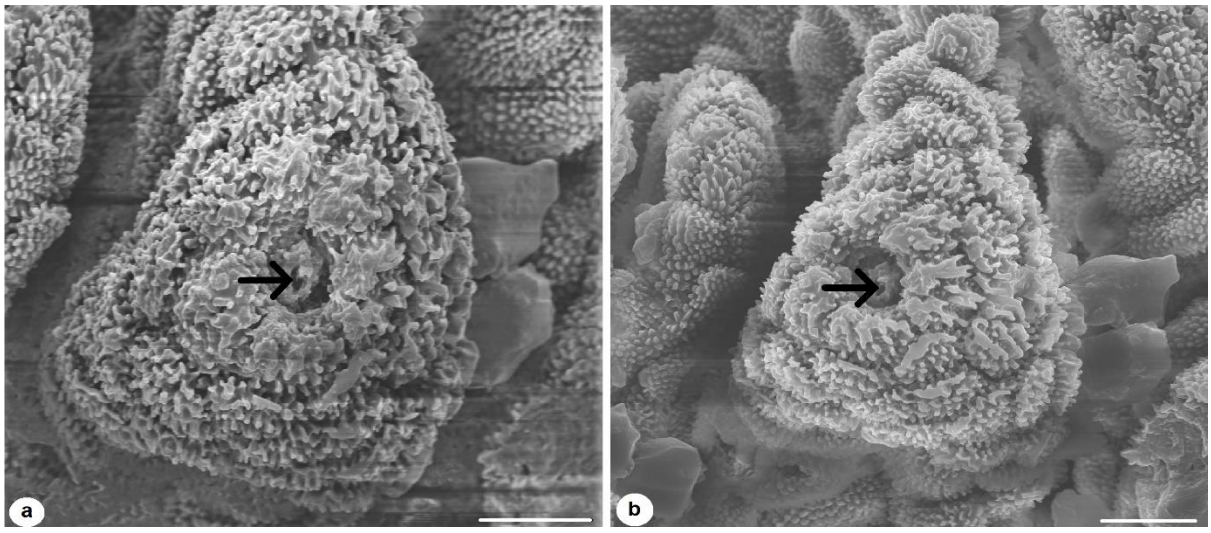

Figure 9. Anterior accessory gland, character state 2. (a) Heathcote, AM.CC.1, left oncopod, male, 1.1 mm HWE, scale 10 µm. (b) Same specimen from Heathcote, right oncopod, male, scale 10 µm. Arrows indicate distal openings.

3, Fused ribbed papillar scales basally, ribbed distal opening. (Macquarie Pass National Park; Fig. 10a, b).

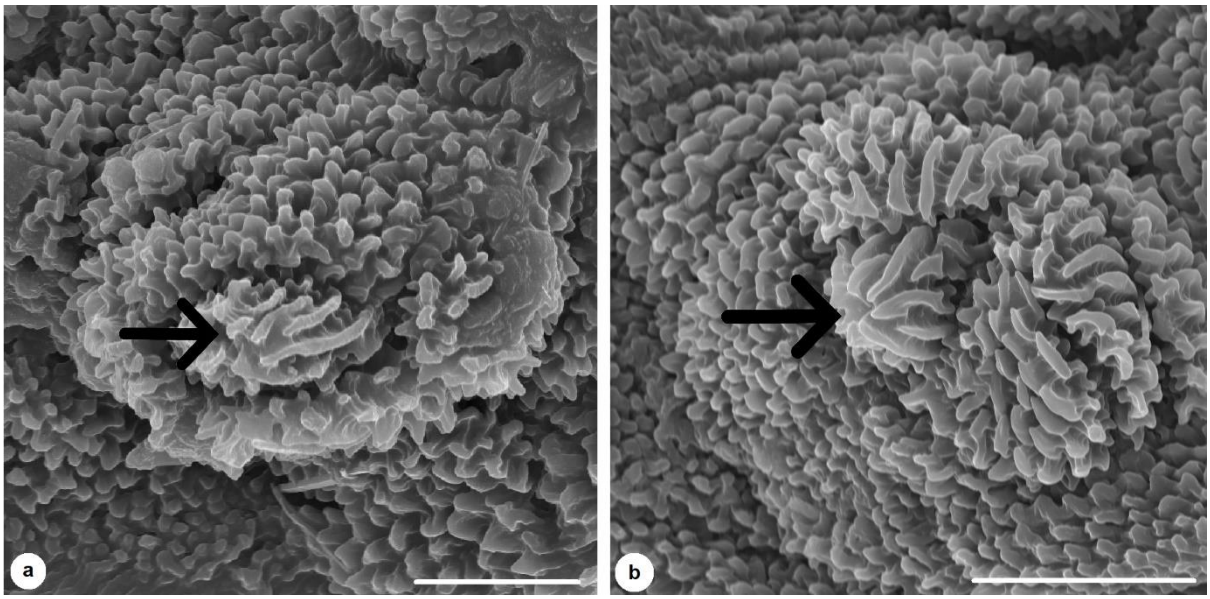

Figure 10. Anterior accessory gland, character state 3. (a) Macquarie Pass National Park, KS.045948, male, 1 mm HWE, scale 5 µm; (b) Macquarie Pass National Park, (different specimen), KS.045948, male, 0.9 mm HWE, scale 5 µm. Arrows indicate distal openings.

4, Ribbed papillar scales basally, with smooth, broad, lip-shaped distal opening (Barrengarry Mountain; Fig. 11a, b).

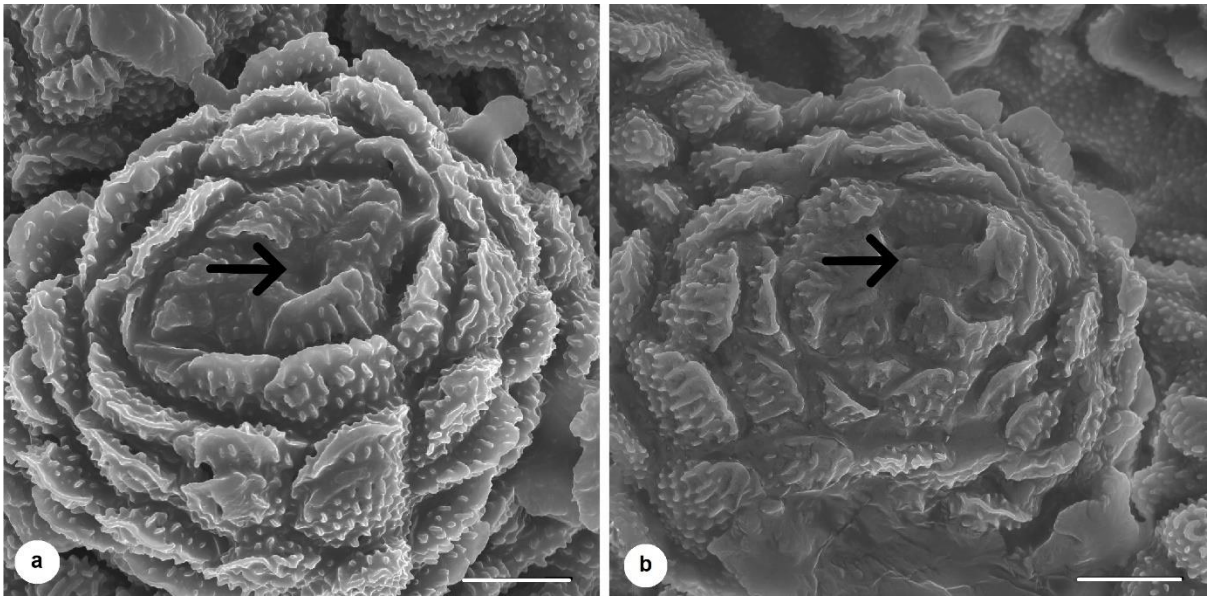

Figure 11. Anterior accessory gland, character state 4. (a) Barrengarry Mountain, KS.119221, male, left, 1 mm HWE, scale 10 µm; (b) Same specimen from Barrengarry Mountain, right, scale 10 µm. Arrows indicate distal openings.

Most populations possessed character state 1: Bundanoon, Mount Gibraltar, Darkes Forest, Mount Keira (i), Mount Keira (ii), Avoca, and Twin Falls. Populations from Heathcote, Macquarie Pass National Park and Barrengarry Mountain each possess character states that were not observed in any other population. This suggests that the ultrastructure of the anterior accessory gland would therefore be successful for identifying and differentiating these populations.

Crural Glands

Crural glands are present on the ventral side of oncopod pairs 2–14 that disperse pheromones to attract male and female conspecifics (Barclay *et al.* 2000). These glands open externally via modified papilla where the glandular secretions are released. Variation was observed in the shape of the distal opening. Two character states were observed:

1, Ribbed papillar scales basally, distal half smooth with long slit-like distal opening (Avoca, Bundanoon, Mount Keira (ii) and Twin Falls; Fig. 12a, b).

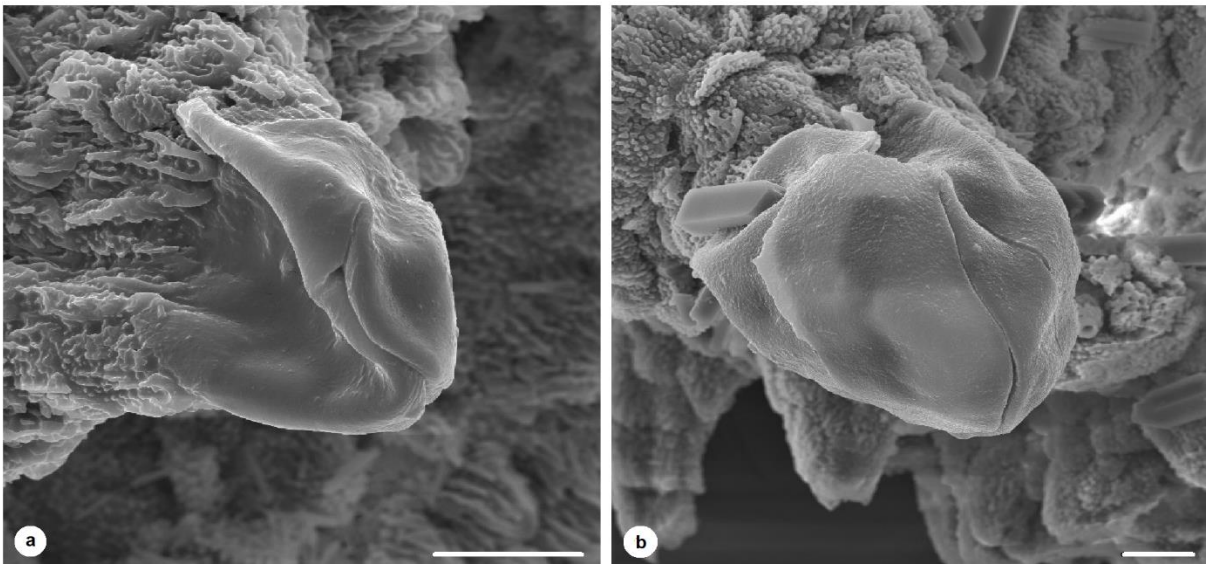

Figure 12. Crural gland on 2nd oncopod pair, character state 1. (a) Bundanoon, KS.16580, male, 1.4 mm HWE, scale 10 µm; (b) Twin Falls, KS.28191, male, 1.2 mm HWE, scale 10 µm.

2, Ribbed papillar scales basally, smooth, narrow, lip-shaped distal opening (Barrengarry Mountain, Darkes Forest, Mount Gibraltar, Macquarie Pass National Park, and Mount Keira (i); Fig. 13a, b).

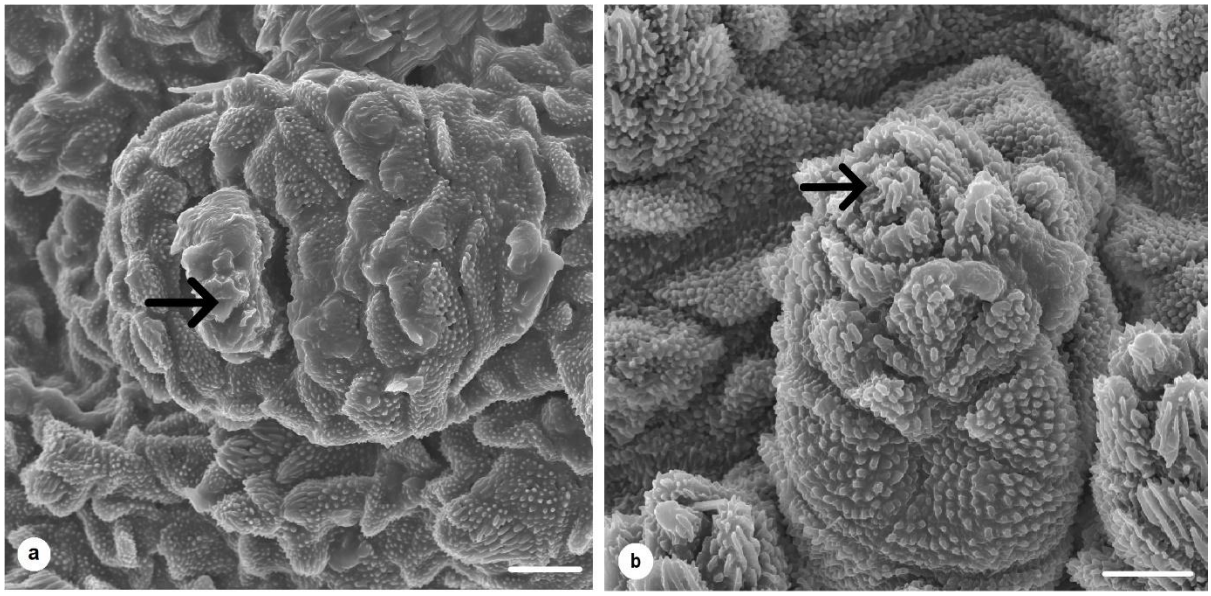

Figure 13. Crural gland on 2nd oncopod pair, character state 2. (a) Barrengarry Mountain, KS.119221, male, 1 mm HWE, scale 10 µm; (d) Macquarie Pass National Park, KS.045948, male, 1 mm HWE, scale 10 µm. Arrows indicate distal openings.

Two character states were observed in the crural gland, each represented by at least four populations. Character state 1: Avoca, Bundanoon, Mount Keira (ii) and Twin Falls populations; character state 2: Barrengarry Mountain, Darkes Forest, Mount Gibraltar, Macquarie Pass National Park, and Mount Keira (i) populations. It should be noted that both characters states were observed in specimens collected from the type locality of *Anoplokaros keerensis* (Mount Keira (i) and (ii)) so this trait may be used to assist in the identification of males collected at this location.

Genital Openings

The genital opening (or gonopore) is the site of the opening to male and female reproductive tracts. Variation was observed in the nature of fusion of the papillae surrounding the genital opening, as well as the concentration of the mechanoreceptive spines. Two character states were recognised:

1, Low, rounded, not markedly protuberant composed of large partially fused papillae around cross-shaped opening. (Bundanoon, Mount Keira (i), Mount Keira (ii), Avoca, Darkes Forest, Macquarie Pass National Park, Austinmer, Heathcote, Barrengarry Mountain, and Mount Gibraltar; Fig. 14a, b).

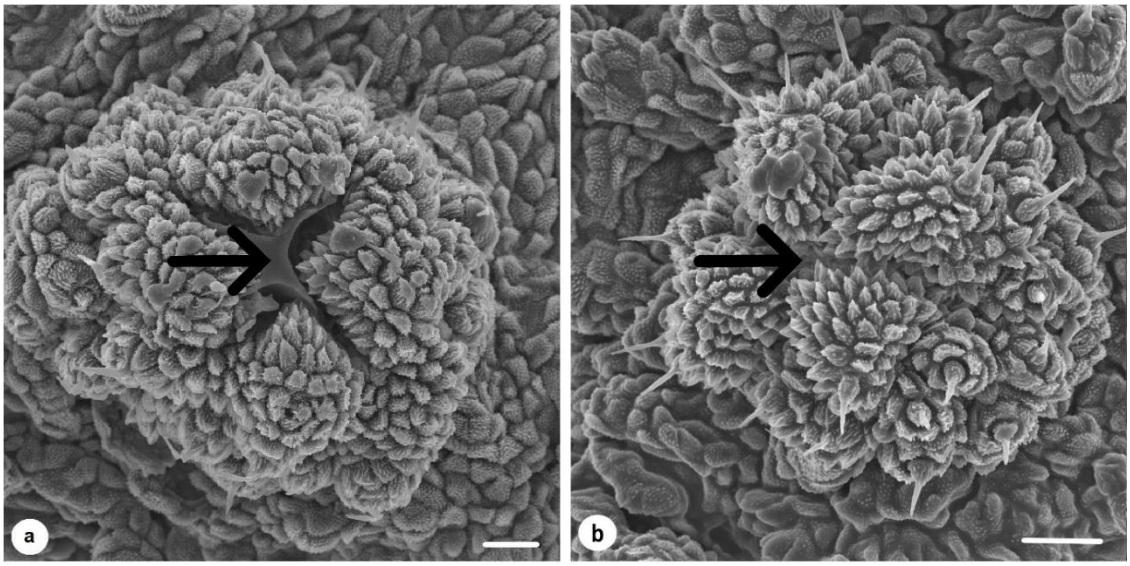

Figure 14. Gonopore, character state 1. (a) Mount Gibraltar, AM.CC5, fresh-collected male, 1.1 mm HWE, scale 10 µm; (b) Barrengarry Mountain, KS.119221, male, 1 mm HWE, scale 10 µm. Arrows indicate openings.

2, Gonopore papillae discrete, less fused, with long spines. (Budderoo National Park; Fig. 15)

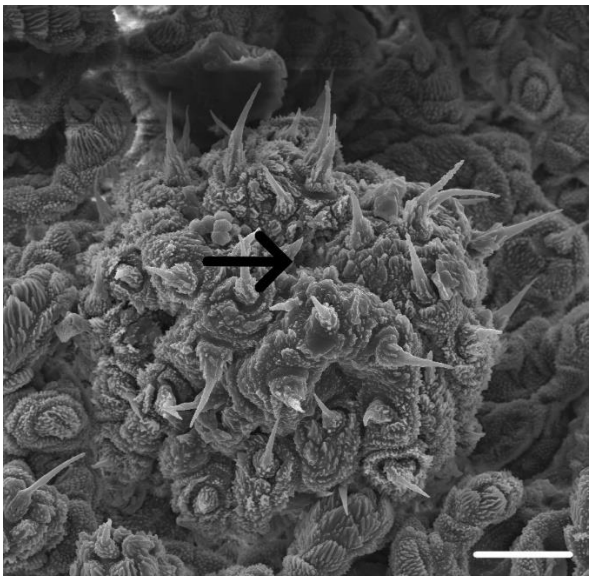

Figure 15. Gonopore, character state 2. Budderoo National Park, AM KS.119248, male, 1.1 mm HWE, scale 10 µm. Arrow indicates opening.

There was no variation observed between males and females. Character state 1 was observed in all populations, except for Budderoo National Park. Therefore, this can only be useful when identifying Budderoo National Park specimens.

Nephridiopores

The nephridiopores are present in both sexes on the ventral side of oncopod pairs 4 and 5 and are located in the middle of the 4th spinous foot pad. The structures are the openings of an excretory organ, that function in waste elimination as well as possibly moisture uptake. Variation was observed in the structure of these openings. Three character states were observed:

1, Smooth distal openings, distal tip sometimes folded, ribbed basally. (Austinmer, Bundanoon, Barrengarry Mountain, Darkes Forest, Mount Gibraltar, Mount Keira (i), Mount Keira (ii), Macquarie Pass National Park, Royal National Park, and Twin Falls; Fig. 16a, b).

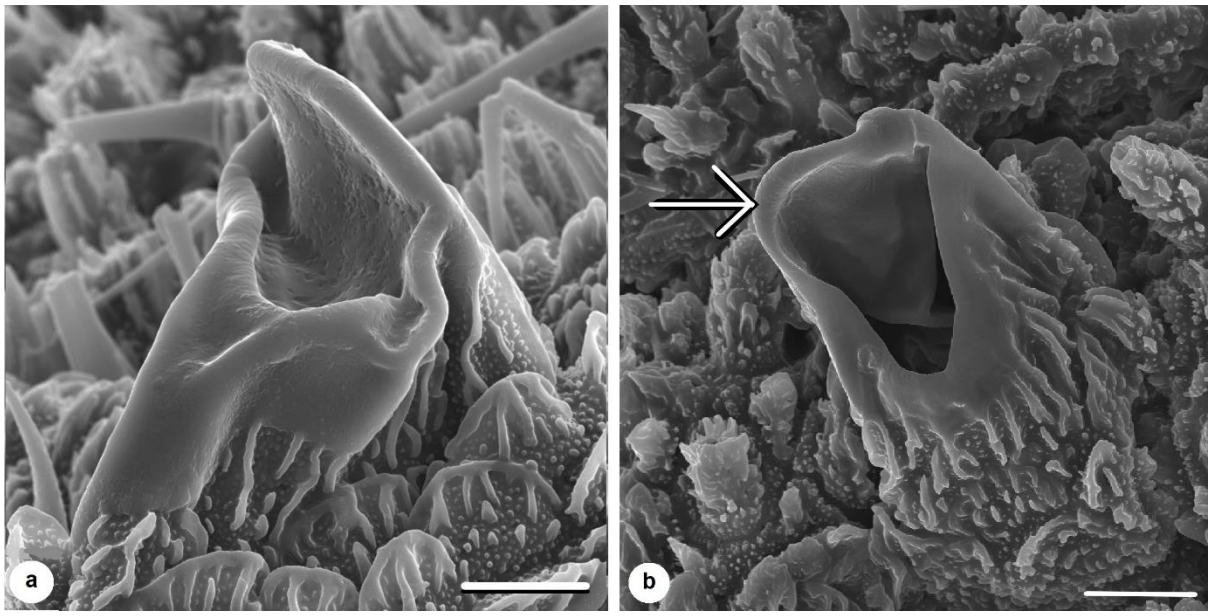

Figure 16. Nephridiopore, character state 1. (a) Austinmer, AM.CC3, fresh-collected female, 1.2 mm HWE, scale 10 µm; (b) Bundanoon, KS.16580, male, 1.4 mm HWE, scale 10 µm. Arrow indicates folded distal tip.

2, Broad and fan-like. Rim smooth on proximal distal margin only (Avoca; Fig. 17a, b).

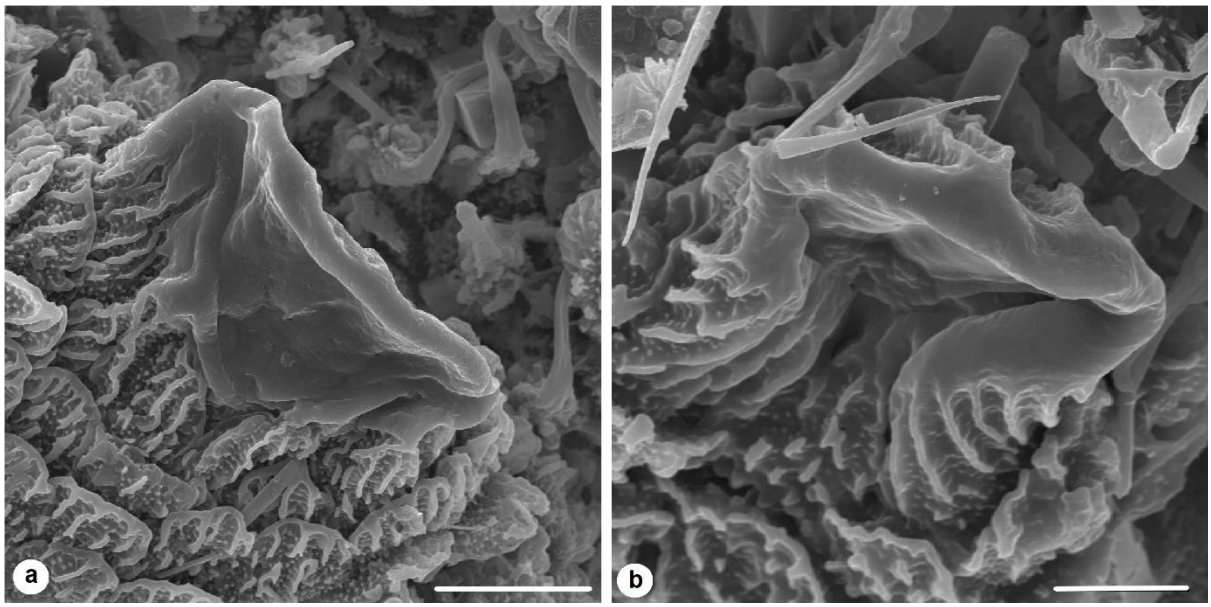

Figure 17. Nephridiopore, character state 2. (a) Avoca, KS.28199, male, 1.3 mm HWE, scale 10 µm; (b) Different specimen from Avoca, KS.28199, opposite view, male, 1.2 mm HWE, scale 10 µm.

3, Smooth, inconspicuous U-shaped opening. (Heathcote; Fig. 18).

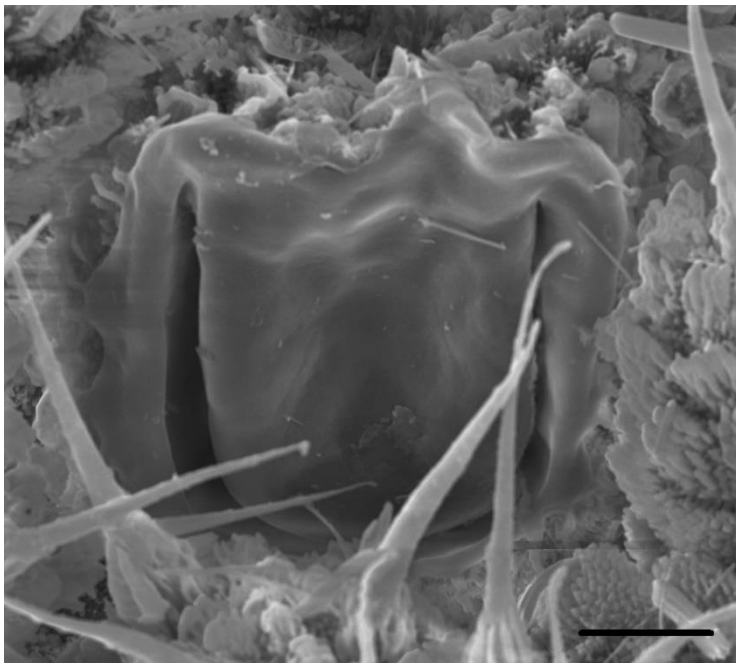

Figure 18. Nephridiopore, character state 3. Heathcote, AM.CC1, male, 1.1 mm HWE, scale 10 µm.

Character state 1 was observed in Austinmer, Bundanoon, Barrengarry Mountain, Darkes Forest, Mount Gibraltar, Mount Keira (i), Mount Keira (ii), Macquarie Pass National Park, Royal National Park, and Twin Falls populations. Character states 2 and 3 were both represented by one population each, Avoca and Heathcote, respectively. Therefore, this character provides diagnostic capabilities in identifying Avoca and Heathcote specimens.

Primary papillae

The dermal integument is covered with primary papillae, that bear mechanoreceptive spines. Within the populations examined, variation was observed in the structure of the primary papillar scales. Four character states were evident.

1, Distal primary papillar scales smooth, or only slightly papillose, and partially fused; basal primary papillar scales ribbed. (Mount Keira (i), Mount Keira (ii), Budderoo National Park, Royal National Park and Austinmer; Fig. 19a, b).

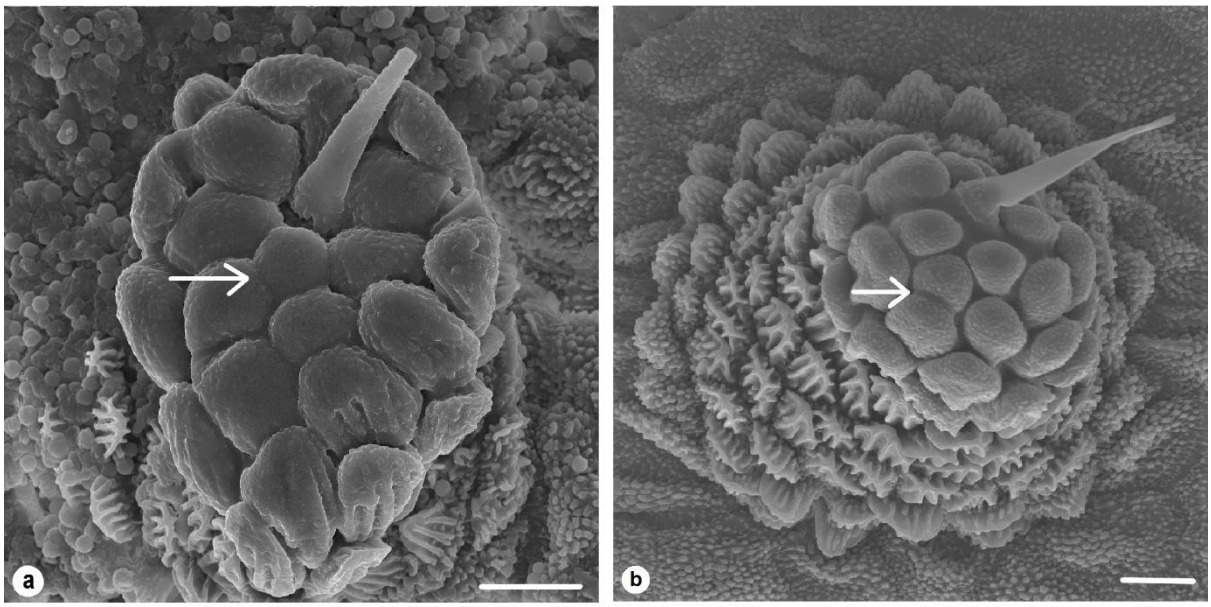

Figure 19. Primary papillae, character state 1. (a) Mount Keira, AM.CC4, fresh-collected male, 1 mm HWE, scale 10 µm; (b) Mount Keira (i), AM.CC4, fresh-collected male, 1.1 mm HWE, scale 10 µm. Arrows indicate examples of fused papillar scales.

2, Distal primary papillar scales clearly papillose, sometimes fused; basal papillar scales ribbed. (Barrengarry Mountain; Fig. 20).

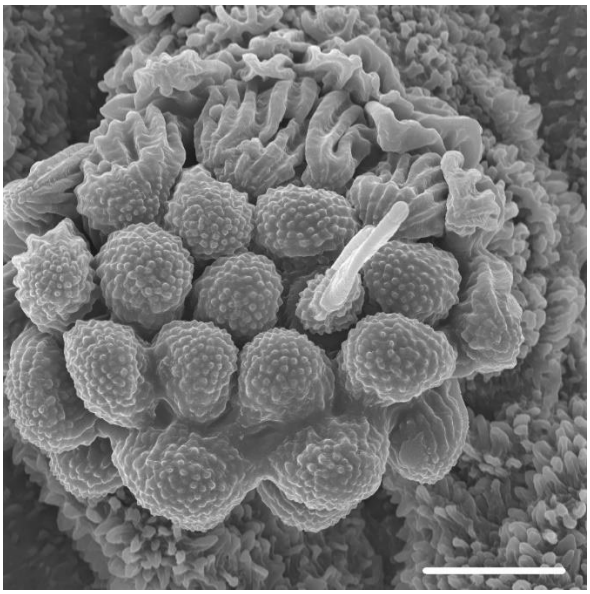

Figure 20. Primary papillae, character state 2. (a) Barrengarry Mountain, KS.119221, female, 1 mm HWE, scale 10 µm.

3, Distal and basal primary papillar scales ribbed*;* not fused. (Macquarie Pass National Park, Heathcote and Mount Gibraltar; Fig. 21a, b).

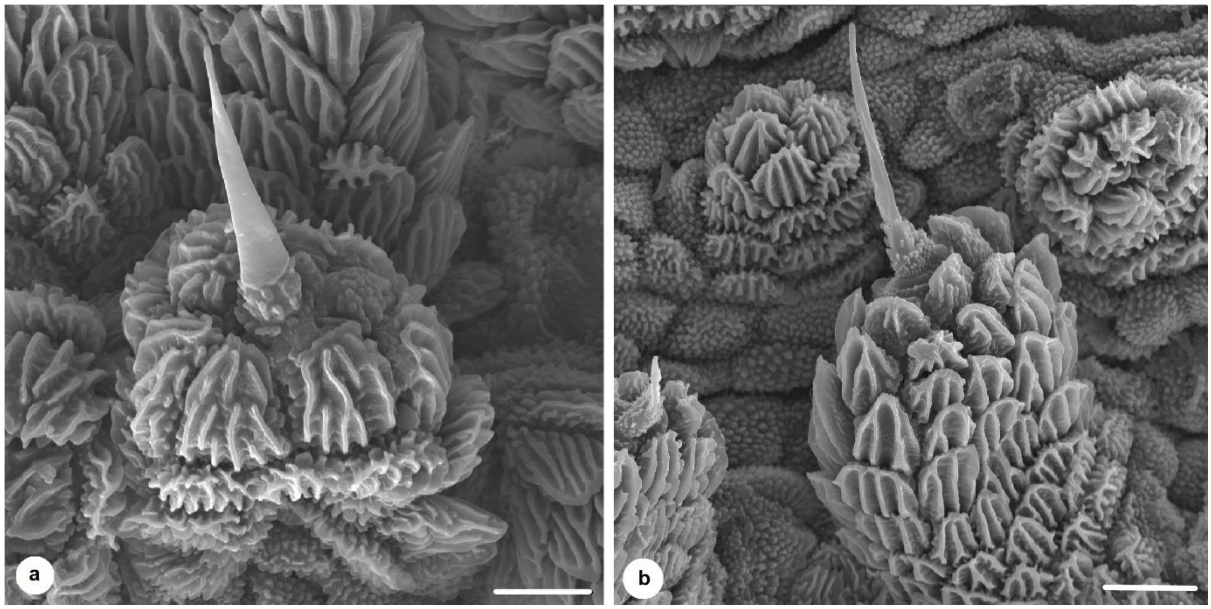

Figure 21. Primary papillae, character state 3. (a) Mount Gibraltar, AM.CC5, fresh-collected male, 1.2 mm HWE, scale 10 µm; (b) Macquarie Pass National Park, KS.045948, male, 1 mm HWE, scale 10 µm.

4, Distal primary papillar scales ribbed basally, ribs partially fused distally, appear crenulated. (Avoca, Twin Falls, Bundanoon, and Darkes Forest; Fig. 22a, b).

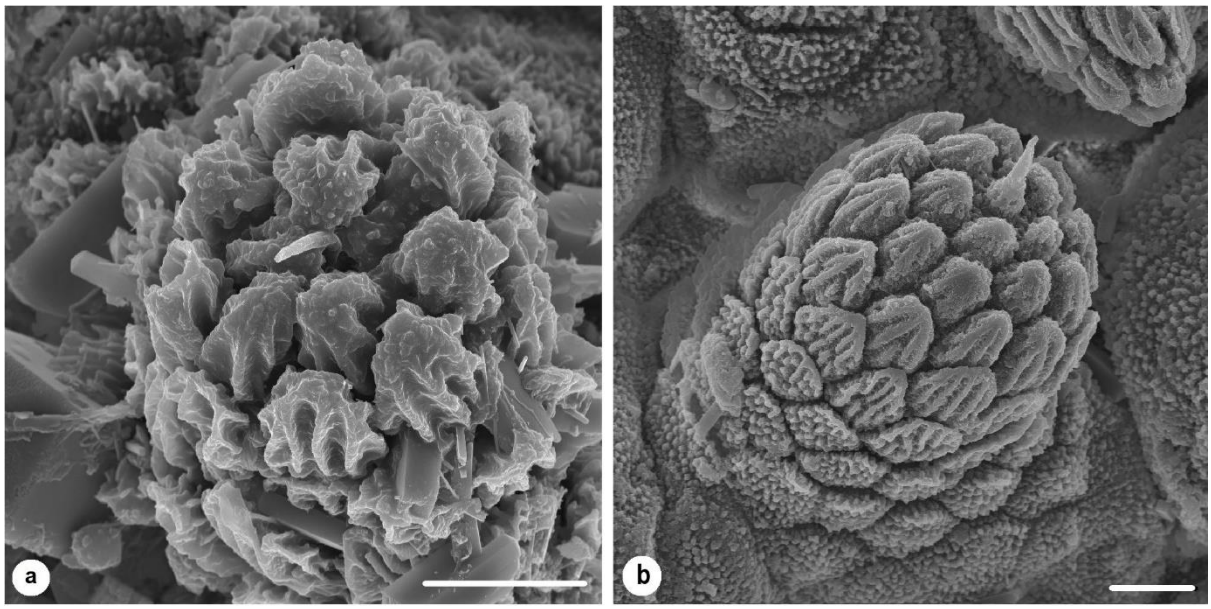

Figure 22. Primary papillae, character state 4. (a) Avoca, KS.28199, male, 1.2 mm HWE, scale 10 µm; (b) Twin Falls, KS.28191, male, 1.5 mm HWE, scale 10 µm.

The primary papillae are the most variable character examined in this study. In summary, among the characters that were examined using SEM, Avoca, Bundanoon and the Twin Falls populations consistently shared the same character states. The specimens from Barrengarry Mountain possessed unique character states in the genital opening, primary papillae and anterior accessory glands that were not observed in any other populations. The specimen from Heathcote also had character states in the nephridiopore and the anterior accessory glands that were not present in any other populations. Notably, Mount Keira (i) and Mount Keira (ii) had the same character states for all the characters examined here, with the exception of the structure of the crural glands.

3.2.3 Internal anatomy

Where available, multiple specimens from each site were examined for notable differences in the shape and size of the internal reproductive organs and associated glands. The only differences observed were in the internal shape and size of the anterior accessory glands. These characters are described below:

Anterior Accessory Glands

1, Moderate length (shorter than posterior accessory glands), cylindrical structures, lying freely within body cavity; without curves or folds. (Avoca, Bundanoon, Twin Falls, Mount Keira (i), Mount Keira (ii), Darkes Forest, Macquarie Pass National Park and Barrengarry Mountain; Fig. 23)

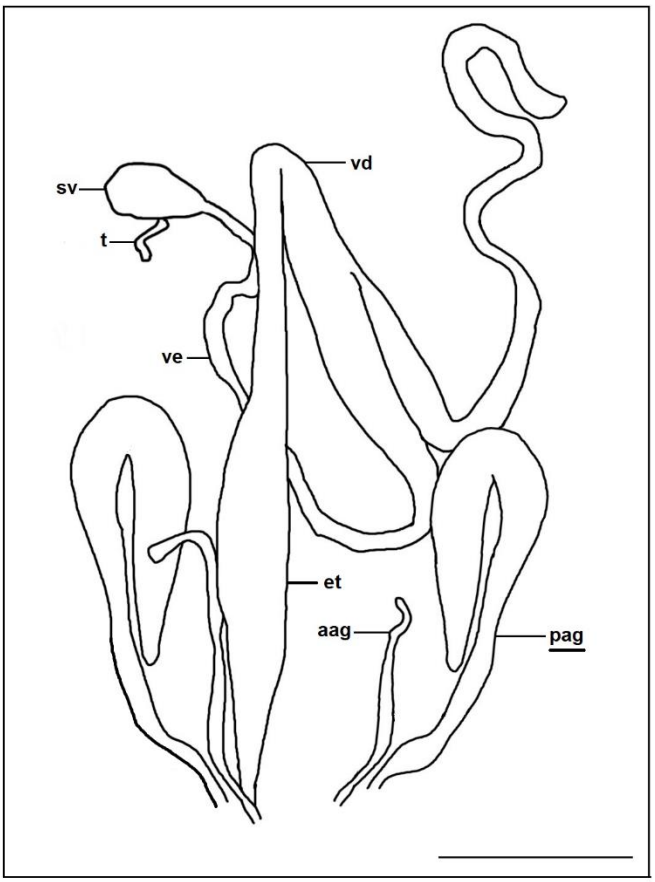

Figure 23. Male reproductive tracts and associated glands; anterior accessory gland, character state 1. Bundanoon, KS.16580, 1 mm HWE, scale 1 mm (only left side testis and seminal vesicle shown). Abbreviations: **aag, anterior accessory gland**; et, ejaculatory tract; pag, posterior accessory gland; sv, seminal vesicle; t, testis; vd, vas deferens; ve, vas efferens.

2, Elongate structure, at least twice the length of the posterior accessory gland, lying freely within body cavity. Irregular, not straight. (Mount Gibraltar; Fig. 24).

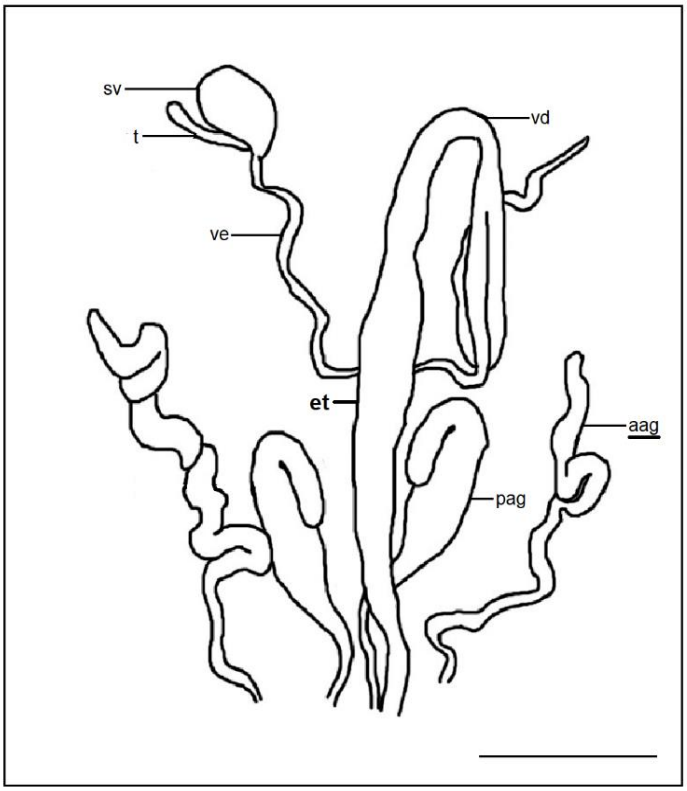

Figure 24. Male reproductive tracts and associated glands; anterior accessory gland, character state 2. Mount Gibraltar, AM.CC5, different specimen, fresh-collected male, 1 mm HWE, scale 1 mm (only left testis and seminal vesicle shown). Abbreviations: **aag, anterior accessory gland**; et, ejaculatory tract; pag, posterior accessory gland; sv, seminal vesicle; t, testis; vd, vas deferens; ve, vas efferens.

Posterior Accessory Glands

Did not differ among specimens examined.

1, Elongated structure, lying freely in body cavity. Distal tip bent posteriorly (Fig. 25).

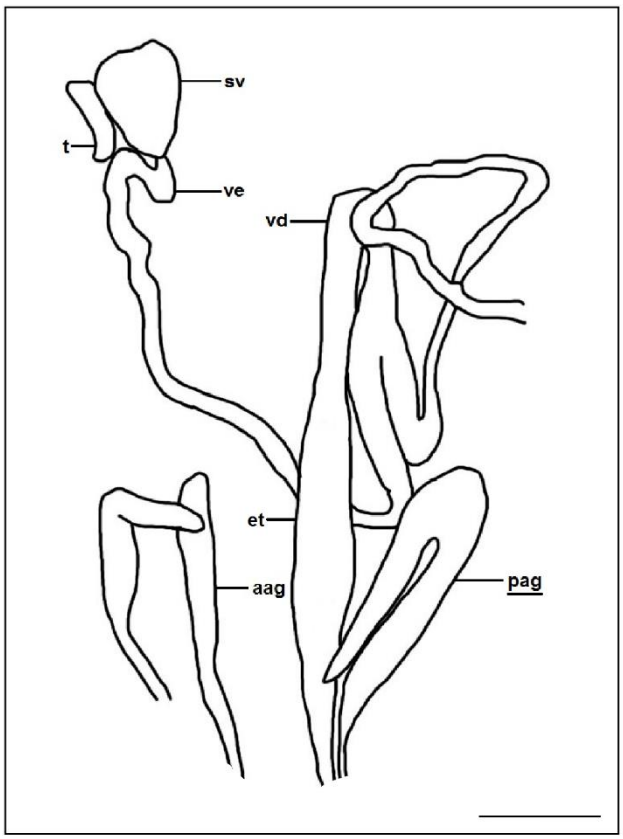

Figure 25. Male reproductive tracts and associated glands; posterior accessory gland, character state 1. Avoca, KS.28199, male, 1.1 mm HWE, scale 1 mm (only left testis and seminal vesicle). Abbreviations: aag, anterior accessory gland; et, ejaculatory tract; **pag, posterior accessory gland**; sv, seminal vesicle; t, testis; vd, vas deferens; ve, vas efferens.

Ejaculatory Tract. There appeared to be one character state present in all specimens. White or pale-pinkish, extending posteriorly towards gonopore (Figs 23–25).

Seminal Vesicle. All specimens appeared to have the same character state. White, opaque globular structures (Figs 23–25).

Testes. There appeared to be no variation in character states between specimens. White or transparent tubular structures, extending posteriorly from seminal vesicle (Figs 23–25).

Vas Deferens. No variation was observed. Walls white and opaque, loops posteriorly towards ejector tract (Figs 23–25).

Vas Efferens. There appeared to be no variation between specimens. Walls thin and white, almost transparent (Figs 23–25).

4. DISCUSSION

This study aimed to utilise integrative techniques to delineate the putative cryptic species-complex *Anoplokaros keerensis*. The molecular analyses provided evidence of genetically discrete clades, suggesting that *A. keerensis* is a complex comprising more than one species. Morphological data somewhat reflected these findings; however, this data type cannot be used as a diagnostic tool in isolation as the morphological data did not seem to outline these genetically discrete clades. This is reflected in several previous studies that also noted cryptic peripatopsid species could not be differentiated by morphological methods alone (Gleeson *et al.* 1998; Trewick 1998, 1999; Daniels *et al.* 2009; Daniels & Ruhberg 2010).

4.1 Molecular analyses

4.1.1 Tissue types

The preliminary tissue studies undertaken revealed that tissue type does not influence the quality of extracted DNA (and subsequent amplified COI sequence fragments) in onychophorans. Several tissue types were tested, including muscle tissue (with and without the presence of adjacent dermal pigments), lateral nerve cord, embryos and ovaries (that had pigments present), and external mouth tissue. These internal tissues, besides the embryos and the dermal tissue, were unpigmented. It appeared that the presence of the dermal pigments did not alter the quality of the extracted DNA or subsequent amplified sequences. This conflicts with the findings of Sunnucks & Wilson (1999) that suggest that pigments may act as PCR inhibitors. As it was determined that several tissue types can produce high-quality sequences, this allowed flexibility when selecting the tissues to be used in extractions, permitting less invasive strategies when undergoing dissections. As onychophorans are cryptic and often hard to find, material for research is sometimes limited. This was found in this study, as well as others such as New (1995) and Chagas-Júnior and Sampaio Costa (2014). Integrative taxonomic investigations rely on material which is used for multiple analyses and therefore needs to be viable for these approaches. If only a single voucher (a specimen that is utilised for a study) is available for a locality or species, it is necessary to use the least invasive methods possible when removing tissues for analyses.

4.1.2 Application of COI to delineate species

The gene region COI was chosen because it has been proven to be among the most conservative mitochondrial protein-coding genes with a high mutational rate, which allows the

detection of discreet divergences even within relatively small well-defined populations (Brown 1985; MacRae & Anderson 1988). Mitochondrial DNA is one of the most widely used regions for invertebrate species delineations as it is usually easy to isolate and amplify, even from poorly preserved specimens (Caterino *et al.* 2000). Additionally, protein-coding genes are conserved and effective as translated amino acid sequences can reveal stop codons which correspond to non-functional sequences (Ingolia *et al*. 2014). The COI gene can be very effective in generating identifications as 95% of species among a variety of animal groups have been shown to possess distinctive COI sequences (Ratnasingham & Hebert 2007). This suggests that COI diagnoses are likely to assist in species determination when dealing with poorly understood taxa, such as onychophorans. However, many studies have revealed that it may be naïve to rely on the sole use of a short sequence to resolve the phylogenies of several distinct taxa (Meier *et al*. 2006; Wiemers & Fiedler 2007).

When determining species boundaries, the strongest support is usually obtained from the analysis of multigene data to attain high phylogenetic resolution. In this study, the use of a single gene, COI, including the 'barcode' region (1816–2518 bp) and 'fragment 3' (2511–2938 bp) produced well-supported clades. Future studies, however, should include at least one other gene to increase phylogenetic resolution, such as the ribosomal gene 18S, that has previously been employed for exploring species delineations within the Peripatopsidae (Daniels *et al*. 2009; Ruhberg & Daniels 2013; Oliveira & Mayer 2017).

4.1.3 PCR and Sequencing

Extractions, amplifications and sequencing of COI was successful for 11 out of the 14 specimens selected to be included in the phylogenetic analyses. The three unsuccessful extractions, and/or amplifications, could be attributed to museum preservation (up to 20 years) as well formalin fixation, which may have resulted in fragmented or decayed DNA (Dean & Ballard 2001; Do & Dobrovic 2014). These three specimens did not however have any relevant labelling indicating preservation conditions, so it was uncertain whether formalin fixation was used. Extractions were nonetheless attempted for these specimens in case DNA fragmentation would not be an issue. These museum specimens were previously collected from Darkes Forest and Heathcote. Mitochondrial DNA is considered to be easily amplified, especially in invertebrates, as it is abundant in every cell, so it was expected that the majority of amplifications would be successful (Caterino *et al*. 2000).

The COI 'barcode' region was amplified using the universal primers (LCO1490 and HCO2198; Folmer *et al.* 1994). However, for two specimens collected from the same locality (Barrengarry Mountain) it proved to be difficult to amplify this region. Due to time constraints, it was decided to only attempt to amplify the barcode fragment for these two specimens twice, with variations in the annealing temperature. 'Fragment 3' was also easy to amplify for most specimens except for one from Darkes Forest. This is perplexing as the 'barcode' region is a larger fragment that was successfully amplified. For the other populations, the inclusion of 'fragment 3' provided supplementary genetic material to analyse in addition to the 'barcode' region. Regardless of the inability to amplify some fragments, overall amplification success rate was high, and several specimens had sufficient sequence data to be used in phylogenetic analyses.

The primer pair HCOoutout/LCO1490 was initially used to amplify 'fragment 2' (1816–2668 bp), that would have overlapped 'fragment 3' and provided a continuous COI fragment when concatenated. Difficulties arose when attempting to amplify this 850 bp fragment with the reverse primer (HCOoutout) that subsequently replaced by HCO2198. Although the concatenation of the barcode region (amplified with LCO1490/HCO2198, 1816–2518 bp) and 'fragment 3' resulted in a 43 bp gap between fragments, this was selected for use as the 'barcode' region had already been amplified for the preliminary tissue comparison and thus was known to be successful. The lack of success of the primer HCOoutout was unexpected as it had successfully used to amplify mtDNA from various taxa including Arachnida and Hymenoptera (Schulmeister 2003; Prendini *et al*. 2005; Sharma & Giribet 2009). HCOoutout is a degenerate primer, meaning it is a mixture of primers that contain ambiguous base pairs at numerous sites, allowing those positions to bind more than one base (i.e. R can be substituted for A or G). This would make the primer capable of priming the COI region of a wide range of taxa (Zhang & Hewitt 1997). Interestingly, however, this primer did not bind to onychophoran DNA suggesting that the degeneracy did not improve its applicability to this taxon.

4.1.4 Barcode gap analysis: Is sequence divergence outside intra-specific limits?

Examination of the 'barcode' gap analysis, using the Kimura two-parameter model, produced sequence divergences between populations and provided a quantitative approach for analysis. The highest mean sequence divergence for the COI locus was 12%, observed in Mount Keira (ii). However, within the five geographically defined populations average sequence distances, (excluding the previously mentioned Mount Keira (ii)) were 2.8% (Mount

Gibraltar), 3.25% (Austinmer), 2.5% (Darkes Forest), 2.9% (Budderoo National Park), 3.17% (Mount Keira (i)), which are all markedly lower than reported intra-specific distances within other peripatopsid taxa (Gleeson *et al.* 1998). Generally, intraspecific COI variation is reported to be significantly higher in species such as *E. rowelli* (12.7%), *Ooperipatellus insignis* Dendy, 1890 (11%), *and Peripatoides novaezealandiae* Hutton, 1876 (7%) (Gleeson *et al*. 1998). Although these values were noted to represent single species, Rockman *et al.* (2001) suggests that these taxa are likely to represent interspecific divergences for species-complexes. According to Hebert *et al.* (2003), it is likely that a COI divergence threshold of 2–4% can be utilised to distinguish species of multiple taxonomic groups from a variety of geographic regions. If this is the case, a value between 2–4% could be considered the COI divergence threshold for onychophorans, as this threshold is already being applied to numerous invertebrate taxa.

Interspecific divergences obtained from barcode analyses have been employed by numerous studies to understand species boundaries among velvet worms (Hebert *et al*. 1991; Gleeson *et al*. 1998; Daniels *et al.* 2009; Ruhberg & Daniels 2013). However, the use of sequence divergence as an indicator for speciation in peripatopsids is a contentious issue as there appears to be no prescribed threshold that indicates species boundaries (Daniels *et al.* 2016). The variability in accepted interspecific divergence threshold may be due to discrepancy in scientific interpretations. As these animals are superficially similar in terms of morphology, it is likely that this may result in a reliance on a sequence divergence to delineate species, rather than integrative approaches. The use of a single taxonomic discipline could therefore cause inconsistencies as there would be a lack of supporting evidence. Furthermore, unusually high intraspecific divergence variability for different species could be present within onychophorans (Daniels & Ruhberg 2010; McDonald & Daniels 2012; Daniels *et al*. 2013). It is thus difficult to determine a straightforward divergence cut-off that can diagnose species boundaries.

One technique for determining an interspecific divergence threshold for particular genera is defined by the 'ten-fold rule', in which the divergence threshold is ten times the mean intraspecific variation to diagnose species boundaries within the genus (Hebert *et al*. 2004). This method could not be employed in this study as only one individual was available for several populations. Assuming that each population within this study is a cryptic species within *A. keerensis,* intraspecific divergence was not able to be determined. Without a precise intraspecific divergence value, it is impossible to calculate interspecific divergence thresholds. In fact, the ten-fold method of designing a threshold has been strongly discouraged and has been said to lack biological support in universally delineating species within the animal

kingdom (Meyer & Paulay 2005; Hickerson *et al*. 2006). In order to completely understand and delineate species within this putative species-complex in the future, this barcode gap analysis will require a larger sample size of each population. According to Frézal and Leblois (2008), DNA barcoding can only provide robust specimen assignment in clades for which the taxonomy is well understood and where the representative specimens are thoroughly sampled.

4.1.5 Assessment of Maximum Likelihood analysis

Bootstrap values are formulated via the assessment of confidence for each clade based on the proportion of instances that phylogeny is replicated (Efron *et al*. 1996; Soltis & Soltis 2003). Confidence estimates of tree topologies are then calculated from these proportions. Clades that have corresponding bootstrap values above or equal to 70 are likely to represent true clades, and bootstrap values that are above or equal to 95 confidently represent true clades (Hillis & Bull 1993; Nei & Kumar 2000).

In this study, the prevalence of high bootstrap values suggests high phylogenetic resolution. It appears that the specimens from northern localities form a clade separate from southern localities. These clades are represented by specimens from Mount Keira (i) and Austinmer (northern clade); as well as Barrengarry Mountain, Budderoo National Park and Mount Gibraltar (southern clade). Further differences were uncovered, the most significant being represented by Mount Keira (ii) which is distinct from all other taxa, as well as a specimen from Darkes Forest branching off with a high bootstrap value (>85).

4.1.6 Implications of phylogenetic analyses

As previously mentioned, the sole use of sequence divergence thresholds for delineating onychophoran species is a contentious issue. Despite this, the combination of the Maximum Likelihood analysis, as well as the ‘barcode’ gap analysis, provided congruent evidence of cryptic speciation within *A. keerensis*. For this study, a divergence threshold of 3% will be used to define species boundaries, with respect to sample size and bootstrap support. This value was selected based on Hebert *et al.* (2003), where a divergence value of 3% was successfully employed as a threshold for species diagnosis. This led to the delinetion of 196 out of the 200 (98%) invertebrate species recognised through prior morphological study. This threshold value has also been widely employed in other invertebrate taxonomic studies for species delineations (Barrett & Hebert 2005; Park *et al*. 2011). On this basis, the presence of three novel species among these populations has been postulated.

The ML analysis results suggested that a clade was present including Mount Keira (i) and Austinmer specimens, which is supported by a mean divergence of 1.8%. The Mount Keira (i) specimens are morphologically identical to the morphological description of *A. keerensis* (Reid 1996). These specimens, along with the Austinmer specimens, have been previously referred to as a 'northern clade' (bootstrap support = 75). The compatibility of both phylogenetic analyses (K2P divergence and ML tree) suggest both Mount Keira (i) specimens the Austinmer specimen represent two populations within *A. keerensis*. The Darkes Forest specimen has a mean divergence of 2.7% from these populations, and also branches from both the northern and southern clade. This is notable as the low divergence value (<3) indicates that the Darkes Forest specimen also represents a population of *A. keerensis*. However, this cannot be determined with absolute confidence, as only one specimen provided the functional sequence. This population should be examined with more specimens.

The 'southern clade' include specimens from Budderoo National Park and Mount Gibraltar (0.9%) as well as Barrengarry Mountain. These three populations diverge from the 'northern clade' and appear to be a species separate from *A. keerensis*, with a mean divergence of 3.8% (bootstrap = 60). The Mount Gibraltar and Budderoo National Park specimens only have a 0.9% sequence divergence, suggesting these two populations likely belong to the same species. The third population within the 'southern clade', Barrengarry Mountain, may be a separate species to the Mount Gibraltar and Budderoo National Park populations, supported by a high bootstrap value (99) and long branch length (Fig. 4).

Finally, the Mt Keira (ii) specimen collected from the type locality notably branched separately from all other specimens. The high mean divergence of 12%, along with a long branch length, suggests that this specimen belongs to a novel species. However, a solid conclusion cannot be drawn as only a single specimen is representative of this divergence value. Furthermore, this specimen was collected from a woodpile that could have possibly been imported from another site. To determine with a higher degree of confidence whether this in fact a separate species, freshly collected material from Mount Keira needs to be examined.

4.2 Morphological Analyses

4.2.1 Application of Morphology

Within this study, several morphological features with previously recognised diagnostic utility were assessed to discriminate between specimens collected from various locations around the Illawarra region. Body pattern and colouration were both highly conserved as all

taxa exhibited a repeating pattern of short, dark, blotches present dorsally at every oncopod pair with light patches, extending from these dark blotches along mid-dorsal line transversely, that convex posteriorly. Scanning electron micrographs revealed a number of differences in morphology, with the sculpture of the dermal primary papillar scales and crural glands being the most distinctive characters. The posterior accessory gland morphology also differed between specimens, as well as the external structure of the anterior accessory gland. There is significant morphological variation among supposed '*A. keerensis*' but this was not completely congruent with the observed molecular variation making it difficult to draw firm conclusions about meaningful taxon boundaries.

4.2.2 Body colour and pattern

Two colour morphs were observed within the majority of the populations, including Mount Keira, Darkes Forest, Mount Gibraltar, Bundanoon, Avoca, and Twin Falls. Specimens either possessed dominant blue and black dermal pigmentations, or, more commonly, brown and black pigments. In the blue-black colour morphs the repeated body pattern was obscured by the dark background colouration and less distinctive. This has also been observed in numerous other peripatopsids, including *Cephalofovea* Ruhberg, Tait, Briscoe and Storch, 1988, species (Reid *et al*. 1995). These colour morphs were observed in both sexes, suggesting that this trait is not sex-linked dimorphisms and more likely to be random morphotypes. The evolutionary advantage of the various colour morphs (if of any advantage at all) within populations is unclear. These animals spend the majority of their time in coarse woody debris and leaf litter, suggesting colouration would play a role in crypticity through camouflage (Read & Hughes 1987). However, how these colours and patterns are perceived by predators, conspecifics and other onychophorans is largely unknown. Interestingly, onychophorans are most sensitive to light within blue wavelengths which may explain why blue pigments are present, despite their poor vision (Beckmann *et al*. 2015). There does not appear to be any variation in body pattern among the geographically separate populations, suggesting that this characteristic does not reflect species boundaries.

4.2.3 Scanning Electron Microscopy

Within this study, five morphological characters were examined between specimens from different populations. Numerous character states were observed, although little correlation between localities and morphology was seen. The nature of the scalation of the

primary dermal papillae appeared to be the most diagnostic. The application of this character has previously and successfully been used to the presence of cryptic species, particularly among closely related groups or within species-complexes (Read 1988; Oliviera *et al*. 2010).

Primary dermal papillae have a distal spine or bristle extending distally which has mechanoreceptive abilities. The four character states identified in the populations included in this study are defined by the structure or fusing of the papillar scales. The evolutionary significance of the structural form of dermal papillae remains unclear, although seemingly trivial, they may play an important role in several aspects of survival. Velvet worms are desiccation resistant through hydrophobicity which is crucial for survival, so it might be expected that a hydrophobic substance such as wax could be present on the dermal extremities. However, Storch and Ruhberg (1977, 1993) demonstrated that water-repellent substances are not present in the cuticle, suggesting that the hydrophobic nature of onychophorans is a result of the particular structure of these scale-like papillae, as speculated in Oliveira & Mayer (2017). Perhaps the slight differences in scalation seen in this study may reflect the specific microhabitats and physiological requirements of each site which can be used to differentiate each population.

In contrast, the arrangement of the bristles per antennal ring within this putative species-complex were not diagnostic. Members of all populations examined had only one row of bristles per antennal ring. The bristles found on each antennal ring possess mechanoreceptive abilities and enable onychophorans to detect the presence of prey, as well as other onychophorans (Mayer *et al*. 2015). The density and number of spines in the Mount Keira (i) specimen appears to be greater, although, this was only observed in one specimen. This should be examined further in additional specimens. A lack of variance in the shape of the genital opening was observed throughout all populations, besides Budderoo National Park which possessed a distinct character state. This character state appears to possess more mechanoreceptive bristles around the genital opening (Fig. 15). Further morphological analyses should be undertaken, as only a single female specimen was available for this study.

Variation was observed in the morphology of the nephridiopores. It was determined that character state 1 was observed in the majority of specimens (Fig. 16a, b), whereas character states 2 and 3 were observed in only one population each (Avoca and Heathcote; Figs 17a, b and 18, respectively). The anterior accessory gland micrographs also revealed that character state 1 was observed in the majority of populations where character states 2, 3 and 4 were each represented by one population each (Heathcote, Macquarie Pass National Park and Barrengarry Mountain; Figs 9a, b, 10a, b and 11a, b, respectively). The function of the anterior accessory

glands is unknown, but they are assumed have some role in reproduction or the production of pheromones (Reid 1996).

The crural glands are located on the ventral side of oncopod pairs 2 to 14 in males and have been said to secrete pheromones that play a role in dispersal, as well as reproduction on onychophorans (Eliott *et al*. 1993). These glands come into contact with the substrate as velvet worms are moving around and deposit pheromone trails which attract both male and female conspecifics (Barclay *et al*. 2000). The two character states observed within these populations allowed some diagnostic abilities, as each character state was represented by geographically adjacent populations. Character state 1 was observed in Avoca, Bundanoon, Twin Falls and Mount Keira (ii) specimens, whereas character state 2 was observed in Darkes Forest, Mount Keira (i), Mount Gibraltar, Barrengarry Mountain, Heathcote and Macquarie Pass National Park populations. Notably, the crural gland was the only character that could be used to distinctively distinguish Mount Keira (i) and (ii).

4.2.4 Internal anatomy

The reproductive organs and associated glands, such as the anterior and posterior accessory glands of male specimens were examined in terms of the shape and structure. The only variation was observed in the anterior accessory gland. As previously mentioned, the role of this gland is unknown, but it may secrete reproductive pheromones (Reid 1996). Character state 1 was observed in all specimens except for the Mount Gibraltar population, in which character state 2 was observed. Despite this, the posterior accessory gland, ejaculatory tract, seminal vesicle, testis, vas deferens and vas efferens all offered no diagnostic potential. The anatomical data obtained did not seem to reflect the molecular data and offered limited diagnostic capabilities. However, the internal structure of the anterior accessory glands of the Mount Gibraltar population can be used to differentiate these specimens from others. Overall, these results suggest that these characters cannot be used to understand the taxonomic status of *A. keerensis.*

4.2.5 Implications of morphology

The specimens from Avoca, Twin Falls, Bundanoon, Royal National Park, Heathcote and Macquarie Pass National Park do not have any relevant molecular data to compliment the morphological data presented within this study and therefore are excluded from discussion in the ‘integrative taxonomy’ section below. The comprehensive morphological descriptions

provided in the Appendix could be used as a baseline to facilitate future investigations of these populations. The morphological variations observed suggest that further integrative studies should be undertaken to understand their taxonomic status.

Specimens from Bundanoon, Avoca and Twin Falls all appear to consistently possess the same character states for four out of five morphological characters examined. These three populations appear to represent a morphotype within *A. keerensis*. Furthermore, the female specimen from the Royal National Park possessed three of the same character states as the *A. keerensis* type specimens. As there were no male specimens available, it is difficult to determine whether this population is morphological identical to *A. keerensis* from the type locality.

The Heathcote specimen was observed to possess unique character states in the anterior accessory gland and nephridiopore, that were not represented by any other populations. As only one specimen was available from this site, a larger sample size should be used to further examine these notable differences. The Macquarie Pass National Park specimens also possessed a character state in the anterior accessory gland that was not observed in any other populations. It is unfortunate that these populations could not be examined any further, as these unique morphological traits could represent further taxonomic divisions within supposed *A. keerensis*.

4.3 Integrative taxonomy

Congruence between the two molecular analyses ('barcode' gap analysis and Maximum Likelihood) suggests that multiple species are nested within populations previously attributed to *A. keerensis,* reflected by some morphological variation and geographic isolation. These species seem to be represented by: 1) Mount Gibraltar and Budderoo National Park populations, 2) Barrengarry Mountain population, 3) Mount Keira (ii). Furthermore, it was determined that the specimens collected from Darkes Forest and Austinmer, as well as Mount Keira (i) specimens, are populations within *A. keerensis*, although this should be examined with more material.

The morphological assessment of the female specimen collected from Austinmer reflects these molecular results, in that this specimen is morphologically similar to the *A. keerensis* type specimens (Mount Keira (i)). However, there was only one female available from this site and therefore morphological comparisons of the male-specific characters, such as the crural gland and anterior accessory gland, could not be undertaken. The Darkes Forest

specimen was also said to represent a population within *A. keerensis*, possessed slight morphological variation from the type specimen in the crural gland and primary papillae. These two populations should be examined further, when more specimens become available.

The Mount Gibraltar and Budderoo National Park specimens were previously noted to belong to a novel species within the molecular analyses, which is somewhat reflected by morphology as differences in the primary papillae and genital opening were observed. The Barrengarry Mountain specimens morphologically differed from these two populations which is supported in the molecular analyses. Finally, the two genetically distinct populations from Mount Keira (i) and (ii) seemed to only vary slightly in morphology, as they possessed different character states for the crural gland. These integrative results are notable as populations with a divergence of 0.9% (Budderoo National Park and Mount Gibraltar) appear to have more morphological distinctiveness than populations with a 12% divergence (Mt Keira (i) and (ii)).

The primary papillae character states were plotted against each population, as the most variation was seen in this character. As seen in Figure 26, the primary papillae morphology somewhat reflects the results of the molecular analyses, although within clade variation exists. It appears that character state 1 can be used to identify Mount Keira, Austinmer and Budderoo National Park populations, which are notably quite close geographically. Furthermore, the Darkes Forest specimens possess a distinctive character state (4), which is reflected by the ML tree as it branches from the clades. The 'southern clade' populations, Mount Gibraltar, Barrengarry Mountain and Budderoo National Park, all have different character states, making this character unable to definitively diagnose this clade from the other.

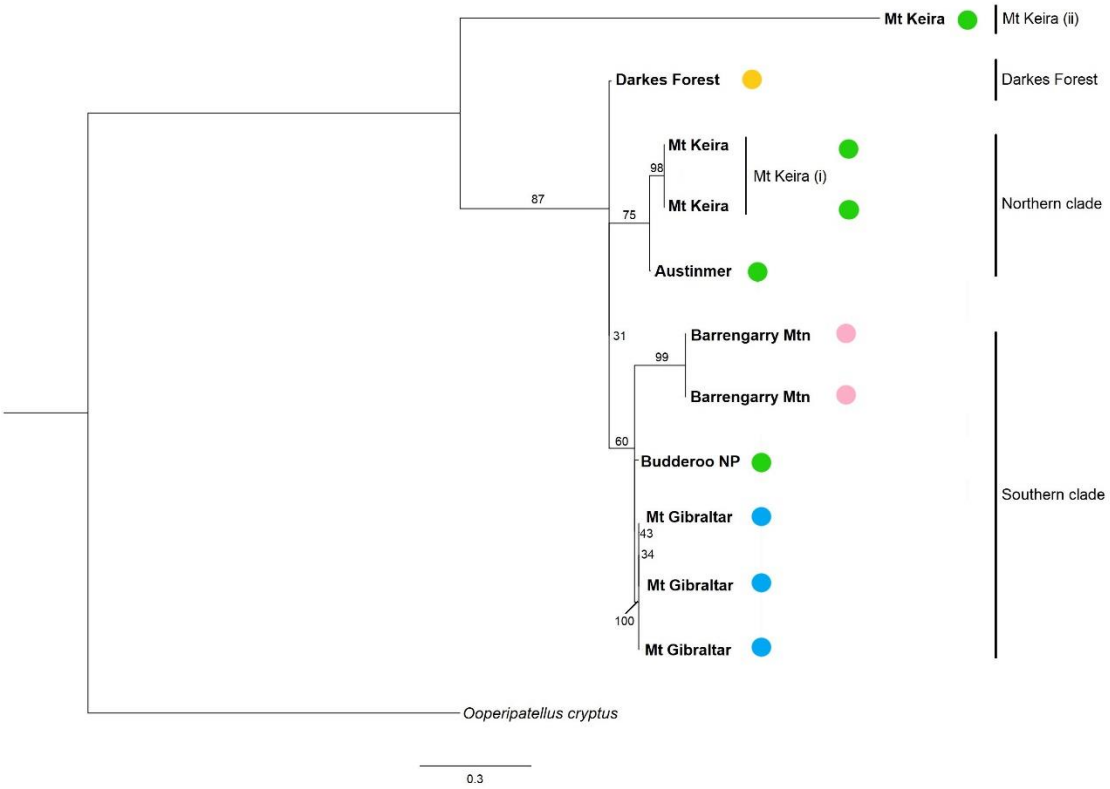

Figure 26. Phylogenetic relationships among specimens examined, including the outgroup, O. cryptus. Maximum Likelihood tree constructed from COI nucleotide sequences. Node labels indicate bootstrap support. Bootstrap iterations = 500. Each primary papillae character state represented by a colour: green (character state 1), pink (character state 2), blue (character state 3) and yellow (character state 4).

The use of integrative taxonomic methodologies provided evidence for widespread cryptic speciation within *Anoplokaros keerensis*, previously undetected using conventional morphology-based taxonomy (Reid 1996). The studied morphology doesn't definitively align with the COI results, suggesting further analyses should be undertaken to understand the taxonomic status of the distinct populations recognised in this study. Future analyses could include behavioural studies which may provide a more in-depth taxonomic understanding and thus aid in species delineations. Despite this, morphology has previously proven to be useful in discriminating between groups of onycophoran taxa, such as in Rockman *et al.* (2001) where the head structures found on males definitively represented phylogenetic clades in *Planipapillus* species. Although this character can differentiate species within *Planipapillus*, it may not be applicable to all onychophoran species (Daniels *et al.* 2009), such as the one presented in this study.

Morphology is a widely use taxonomic approach used to distinguish species, although in morphologically conserved taxa such as onychophorans, other approaches should be considered (Dayrat 2005). These approaches could include behavioural, phylogeographic,

ecological or developmental studies. It is likely that onychophorans independently evolve to niche habitats in ways we cannot interpret using morphology. For this reason, chemical or protein profiling may be a more appropriate method of species identification and delineation. Slime protein profiling has proven to be a successful non-invasive species identification tool for the two onychophoran families Peripatidae and Peripatopsidae (Baer *et al*. 2014). Additional to this, pheromones could be a valuable method of delineating species, as male pheromonal secretions have been found to be highly attractive to conspecific males and females (Eliott *et al*. 1993; Barclay *et al*. 2000). These chemicals play a major role in reproduction and dispersal in that they are likely to be species-specific. These alternative methods of species diagnosis may be a more efficient way to fully understand the *Anoplokaros* genus. Onychophoran fossil records indicate that their morphology has changed relatively little over the past 300 million years, suggesting it may be naïve to use this as a delineating tool (Liu *et al.* 2008). The morphology results presented in this study suggests that alternative morphological characters need to be investigated in future analyses of this group, or alternative analyses that can complement molecular data. The conserved morphology within the phylum Onychophora is likely to have contributed to the underestimation of species diversity within Australia.

It would be expected that historical biogeography plays a major role in genetic structuring among onychophorans, as these animals are restricted to small habitats creating high occurrences of point endemism (Rockman *et al*. 2001). The diversity observed between the onychophoran populations examined could be a product of historical peri-glaciation cycles on the east coast of Australia (Garrick *et al*. 2004). Peri-glaciation refers to geomorphic processes that results in seasonal freezing and thawing (Bowler *et al.* 1976). These events would have caused significant habitat reorganisation, resulting in refugees becoming re-established when conditions allow the restoration of viable habitat (Porter 1999). Paleoclimatic influences could have also resulted in the geographical divisions of the 'northern' and 'southern' clades we see today.

As these animals exhibit one the most extreme forms of short-range endemism, they are highly dependent upon specific microhabitat conditions for survival (Harvey 2002). Their limited dispersal capabilities are driven by discontinuous habitats and high vulnerability to desiccation (Bull *et al*. 2013). Therefore, large-scale human-induced changes have significant impacts on these small geographic ranges. In fact, whilst attempting to collect specimens previously found at Avoca, a small town in the Southern Highlands, it was discovered that little to no forest was left surrounding the town as it had been cleared and converted into paddocks.

Habitat destruction and deforestation, such as this event of extensive land clearing, has the potential to eradicate entire species (Debinski & Holt 2000; Fahrig 2003). Unfortunately, there have been several onychophoran species that have become endangered or extinct in recent years because effective conservation policies could not be enacted as fast as their habitats were disappearing (Brinck 1957; Hamer *et al.* 1997; Jackson & Taylor 1994; Daniels 2011; Oliveira *et al.* 2015).

Invertebrate conservation is often challenging when targeting specific taxa, rather than a habitat or ecosystem (Lewinsohn *et al*. 2005). Charismatic or flagship species are species that are selected to act as an icon for a defined habitat to represent conservation or an environmental issue. In fact, a species of velvet worm, *Epiperipatus acacioi* Marcus & Marcus 1955, was used as a flagship species to conserve a small patch of forest in Brazil (Oliveira *et al.* 2015). Not only can onychophorans be used to justify the preservation of a particular habitat, they may also indicate high species richness. As these animals are short-range endemics, the underlying ecological processes that assisted in the retention of these species may have also initiated speciation events in multiple other taxa, creating biodiverse endemic hot-spots. Furthermore, habitat degradation will only worsen the prospects for long-term survival of taxa that are restricted to small habitats (Fahrig 1997).

5. CONCLUSIONS

This study provides further evidence that the populations previously attributed to the taxon *Anoplokaros keerensis* likely comprise of more than a single species. The evaluation of the taxonomic status of this putative cryptic-species was undertaken with the use of the mitochondrial gene COI using Maximum Likelihood analyses and Barcode gap analysis in addition to morphological data. The integration of molecular and morphological analyses enables taxonomic insight into cryptic and poorly understood taxa, thus making studies such as this of great importance.

As the use of ‘barcode’ gap to generate standardised divergence thresholds to delineate species is a contentious issue, it was difficult to determine with confidence whether several species had in fact been amassed under one name. To investigate this further, a Maximum Likelihood analysis was performed. These results supported the barcode gap analysis providing more evidence of cryptic speciation. The Mount Keira (i) and Austinmer specimens (‘northern clade’) were morphologically identical to the type specimens. The Austinmer specimen also appeared to be genetically similar to *A. keerensis,* along with the Darkes Forest specimen, although this population varied slightly in morphology. It was also determined that a novel

species is present at the *A. kerensis* type locality, Mount Keira, although it is uncertain whether this species had been introduced by importing wood or occurs naturally at this location (the presence of more than one species at a location is not unusual among onychophorans). Additionally, the Mount Gibraltar and Budderoo National Park specimens appear to belong to a putative novel species, as well as the Barrengarry Mountain specimens, suggesting that there may be two novel species within the 'southern clade'. Further research will have to be conducted to test the species hypotheses suggested here.

The morphological variation represented in this study was not reflected by the morphological analyses. The populations examined using morphology alone, including Bundanoon, Avoca, Twin Falls, Royal National Park, Heathcote and Macquarie Pass National Park varied from *A. keerensis* from the type locality. Further investigation would be useful should fresh material become available. It is crucial to understand the taxonomy and biodiversity of the onychophoran phylum to shed light on the evolutionary complexity and diversity of extant panarthropodal relatives, as well as to help reconstruct the ancestral arthropod. Without comprehensive taxonomic studies such as this, the biodiversity of cryptic taxa would be unknown and thus be excluded from conservation policies. The putative novel species presented within this study, as well as most of the populations examined are fortunately located within protected forested areas, such as National Parks are Nature Reserves. The two populations that are not located within these protected areas include Austinmer and Avoca, which are both subject to progressive human activities such as land development. The presence of these populations justifies the preservation of these particular habitats, as these animals are extremely vulnerable to habitat degradation, and may also indicate high levels of local biodiversity.

REFERENCES

Avise, J. C. and Walker, D. (1999). Species realities and numbers in sexual vertebrates: perspectives from an asexually transmitted genome. *Proceedings of the National Academy of Sciences*, **96**, 992–995.

Baer, A., de Sena Oliveira, I., Steinhagen, M., Beck-Sickinger, A. G. and Mayer, G. (2014). Slime protein profiling: a non-invasive tool for species identification in Onychophora (velvet worms). *Journal of Zoological Systematics and Evolutionary Research*, **52**, 265–272.

Baer, A. and Mayer, G. (2012). Comparative anatomy of slime glands in Onychophora (velvet worms). *Journal of Morphology*, **273**, 1079–1088.

Barclay, S., Ash, J. and Rowell, D. (2000). Environmental factors influencing the presence and abundance of a log-dwelling invertebrate, *Euperipatoides rowelli* (Onychophora: Peripatopsidae). *Journal of Zoology*, **250**, 425–436.

Barclay, S., Rowell, D. M. and Ash, J. (2000). Pheromonally mediated colonization patterns in the velvet worm *Euperipatoides rowelli* (Onychophora). *Journal of Zoology*, **250**, 437–446.

Barrett, R. D. and Hebert, P. D. (2005). Identifying spiders through DNA barcodes. *Canadian Journal of Zoology*, **83**, 481–491.

Beckmann, H., Hering, L., Henze, M. J., Kelber, A., Stevenson, P. A. and Mayer, G. (2015). Spectral sensitivity in Onychophora (velvet worms) revealed by electroretinograms, phototactic behaviour and opsin gene expression. *Journal of Experimental Biology*, **218**, 915–922.

Bickford, D., Lohman, D. J., Sodhi, N. S., Ng, P. K., Meier, R., Winker, K., Ingram, K. K. and Das, I. (2007). Cryptic species as a window on diversity and conservation. *Trends in Ecology and Evolution*, **22**, 148–155.

Bowler, J., Hope, G., Jennings, J., Singh, G. and Walker, D. (1976). Late quaternary climates of Australia and New Guinea. *Quaternary Research*, **6**, 359–394.

Bray, D., Bagu, J. and Koegler, P. (1993). Comparison of hexamethyldisilazane (HMDS), Peldri II, and critical-point drying methods for scanning electron microscopy of biological specimens. *Microscopy Research and Technique*, **26**, 489–495.

Brinck, P. (1957). Onychophora, a review of South African species, with a discussion on the significance of the geographical distribution of the group. *South African Animal Life*, **4**, 7–32.

Brown, W. (1985). *The mitochondrial genome of animals*. R. J. MacIntyre, New York, USA.

Budd, G. E. and Telford, M. J. (2009). The origin and evolution of arthropods. *Nature*, **457**, 812.

Bull, J. K., Sands, C. J., Garrick, R. C., Gardner, M. G., Tait, N. N., Briscoe, D. A., Rowell, D. M. and Sunnucks, P. (2013). Environmental complexity and biodiversity: the multi-layered evolutionary history of a log-dwelling velvet worm in montane temperate Australia. *PloS ONE*, **8**, e84559.

Cain, A. J. (2014). *Animal species and their evolution*. Princeton University Press, London, England.

Campbell, L. I., Rota-Stabelli, O., Edgecombe, G. D., Marchioro, T., Longhorn, S. J., Telford, M. J., Philippe, H., Rebecchi, L., Peterson, K. J. and Pisani, D. (2011). MicroRNAs and phylogenomics resolve the relationships of Tardigrada and suggest that velvet worms are the sister group of Arthropoda. *Proceedings of the National Academy of Sciences*, **108**, 15920–15924.

Cardoso, P., Erwin, T. L., Borges, P. A. V. and New, T. R. (2011). The seven impediments in invertebrate conservation and how to overcome them. *Biological Conservation*, **144**, 2647–2655.

Caterino, M. S., Cho, S. and Sperling, F. A. H. (2000). The current state of insect molecular systematics: A thriving Tower of Babel. *Annual Review of Entomology*, **45**, 1–54.

Chagas-Júnior, A. and Sampaio Costa, C. (2014). *Macroperipatus ohausi*: redescription and taxonomic notes on its status (Onychophora: Peripatidae). *Revista de Biologia Tropical*, **62**, 977–985.

Collen, B., Böhm, M., Kemp, R. and Baillie, J. E. (2012). *Spineless: status and trends of the world's invertebrates*. Zoological Society of London, London, England.

Daniels, S. R. (2011). Genetic variation in the Critically Endangered velvet worm *Opisthopatus roseus* (Onychophora: Peripatopsidae). *African Zoology*, **46**, 419–424.

Daniels, S. R., Dambire, C., Klaus, S. and Sharma, P. P. (2016). Unmasking alpha diversity, cladogenesis and biogeographical patterning in an ancient panarthropod lineage (Onychophora: Peripatopsidae: *Opisthopatus cinctipes*) with the description of five novel species. *Cladistics*, **32**, 506–537.

Daniels, S. R., McDonald, D. E. and Picker, M. D. (2013). Evolutionary insight into the *Peripatopsis balfouri sensu lato* species complex (Onychophora: Peripatopsidae) reveals novel lineages and zoogeographic patterning. *Zoologica Scripta*, **42**, 656–674.

Daniels, S. R., Picker, M. D., Cowlin, R. M. and Hamer, M. L. (2009). Unravelling evolutionary lineages among South African velvet worms (Onychophora: Peripatopsis) provides evidence for widespread cryptic speciation. *Biological Journal of the Linnean Society*, **97**, 200–216.

Daniels, S. R. and Ruhberg, H. (2010). Molecular and morphological variation in a South African velvet worm *Peripatopsis moseleyi* (Onychophora, Peripatopsidae): Evidence for cryptic speciation. *Journal of Zoology*, **282**, 171–179.

Dayrat, B. (2005). Towards integrative taxonomy. *Biological Journal of the Linnean Society*, **85**, 407–417.

de Sena Oliveira, I., Read, V. M. S. J. and Mayer, G. (2012). A world checklist of Onychophora (velvet worms), with notes on nomenclature and status of names. *ZooKeys*, **211**, 1–70.

Dean, M. D. and Ballard, J. W. O. (2001). Factors affecting mitochondrial DNA quality from museum preserved *Drosophila simulans*. *Entomologia Experimentalis et Applicata*, **98**, 279–283.

Debinski, D. M. and Holt, R. D. (2000). A survey and overview of habitat fragmentation experiments. *Conservation Biology*, **14**, 342–355.

Dendy, A. (1894) Note on a new variety of *Peripatus novaezealandiae*, Hutton. *Transactions of the New Zealand Institute (Zoology)*, **27**, 190–191.

Derycke, S., Fonseca, G., Vierstraete, A., Vanfleteren, J., Vincx, M. and Moens, T. (2008). Disentangling taxonomy within the *Rhabditis* (*Pellioditis*) *marina* (Nematoda, Rhabditidae) species complex using molecular and morhological tools. *Zoological Journal of the Linnean Society*, **152**, 1–15.

Dias, S. C. and Lo-Man-Hung, N. F. (2009). First record of an onychophoran (Onychophora, Peripatidae) feeding on a theraphosid spider (Araneae, Theraphosidae). *Journal of Arachnology*, **37**, 116–117.

Do, H. and Dobrovic, A. (2015). Sequence artifacts in DNA from formalin-fixed tissues: causes and strategies for minimization. *Clinical Chemistry*, **61**, 64–71.

Dugan, K. A., Lawrence, H. S., Hares, D. R., Fisher, C. L. and Budowle, B. (2002). An improved method for post-PCR purification for mtDNA sequence analysis. *Journal of Forensic Science*, **47**, 1-8.

Efron, B., Halloran, E. and Holmes, S. (1996). Bootstrap confidence levels for phylogenetic trees. *Proceedings of the National Academy of Sciences*, **93**, 13429–13429.

Eliott, S., Tait, N. and Briscoe, D. (1993). A pheromonal function for the crural glands of the onychophoran *Cephalofovea tomahmontis* (Onychophora: Peripatopsidae). *Journal of Zoology*, **231**, 1–9.

Fahrig, L. (1997). Relative effects of habitat loss and fragmentation on population extinction. *The Journal of Wildlife Management*, **61**, 603–610.

Fahrig, L. (2003). Effects of habitat fragmentation on biodiversity. *Annual Review of Ecology, Evolution, and Systematics*, **34**, 487–515.

Folmer, O., Black, M., Hoeh, W., Lutz, R. and Vrijenhoek, R. (1994). DNA primers for amplification of mitochondrial cytochrome c oxidase subunit I from diverse metazoan invertebrates. *Molecular Marine Biology and Biotechnology*, **3**, 294–299.

Frézal, L. and Leblois, R. (2008). Four years of DNA barcoding: current advances and prospects. *Infection, Genetics and Evolution*, **8**, 727–736.

Garrick, R., Sands, C. J., Rowell, D. M., Tait, N., Greenslade, P. and Sunnucks, P. (2004). Phylogeography recapitulates topography: very fine-scale local endemism of a saproxylic 'giant'springtail at Tallaganda in the Great Dividing Range of south-east Australia. *Molecular Ecology*, **13**, 3329–3344.

Gleeson, D., Rowell, D., Tait, N., Briscoe, D. and Higgins, A. (1998). Phylogenetic relationships among Onychophora from Australasia inferred from the mitochondrial cytochrome oxidase subunit I gene. *Molecular Phylogenetics and Evolution*, **10**, 237–248.

Hamer, M. L., Samways, M. and Ruhberg, H. (1997). A review of the Onychophora of South Africa, with discussion of their conservation. *Annals of the Natal Museum*, **38**, 283–312.

Haritos, V. S., Niranjane, A., Weisman, S., Trueman, H. E., Sriskantha, A. and Sutherland, T. D. (2010). Harnessing disorder: onychophorans use highly unstructured proteins, not silks, for prey capture. *Proceedings of the Royal Society of London B: Biological Sciences*, **277**, 3255–3263.

Harvey, M. S. (2002). Short-range endemism amongst the Australian fauna: some examples from non-marine environments. *Invertebrate Systematics*, **16**, 555–570.

Hebert, P. D., Billington, N., Finston, T. L., Boileau, M. G., Beaton, M. J. and Barrette, R. J. (1991). Genetic variation in the onychophoran *Plicatoperipatus jamaicensis*. *Heredity*, **67**, 221–229.

Hebert, P. D., Penton, E. H., Burns, J. M., Janzen, D. H. and Hallwachs, W. (2004). Ten species in one: DNA barcoding reveals cryptic species in the neotropical skipper butterfly

Astraptes fulgerator. *Proceedings of the National Academy of Sciences*, **101**, 14812–14817.

Hebert, P. D. N., Cywinska, A., Ball, S. L. and deWaard, J. R. (2003). Biological identifications through DNA barcodes. *Proceedings of the Royal Society of London. Series B: Biological Sciences*, **270**, 313–321.

Hickerson, M. J., Meyer, C. P. and Moritz, C. (2006). DNA barcoding will often fail to discover new animal species over broad parameter space. *Systematic Biology*, **55**, 729–739.

Hillis, D. M. and Bull, J. J. (1993). An empirical test of bootstrapping as a method for assessing confidence in phylogenetic analysis. *Systematic Biology*, **42**, 182–192.

Hutton, F. W. (1876). On Peripatus novae-zealandiae. *Annals and Magazine of Natural History*, **18**, 361–369.

Ingolia, N. T., Brar, G. A., Stern-Ginossar, N., Harris, M. S., Talhouarne, G. J., Jackson, S. E., Wills, M. R. and Weissman, J. S. (2014). Ribosome profiling reveals pervasive translation outside of annotated protein-coding genes. *Cell Reports*, **8**, 1365–1379.

Jackson, J. and Taylor, R. (1994). *North-west velvet worm. Threatened Fauna Manual for Production Forests in Tasmania*. Forestry Practices Board, Tasmania, Australia.

Kimura, M. (1980). A simple method for estimating evolutionary rates of base substitutions through comparative studies of nucleotide sequences. *Journal of Molecular Evolution*, **16**, 111–120.

Kumar, S., Stecher, G. and Tamura, K. (2016). MEGA7: molecular evolutionary genetics analysis version 7.0 for bigger datasets. *Molecular Biology and Evolution*, **33**, 1870–1874.

Lewinsohn, T. M., Freitas, A. V. L. and Prado, P. I. (2005). Conservation of terrestrial invertebrates and their habitats in Brazil. *Conservation Biology*, **19**, 640–645.

Liu, J., Shu, D., Han, J., Zhang, Z. and Zhang, X. (2008). Origin, diversification, and relationships of Cambrian lobopods. *Gondwana Research*, **14**, 277–283.

MacRae, A. F. and Anderson, W. W. (1988). Evidence for non-neutrality of mitochondrial DNA haplotypes in *Drosophila pseudoobscura*. *Genetics*, **120**, 485–494.

Marcus, E. D. B.-R. and Marcus, E. (1955). A new peripatus from Minas Gerais, Brazil. *Anais da Academia Brasileira de Ciencias*, **27**, 189–193.

Mayer, G., Franke, F. A., Treffkorn, S., Gross, V. and de Sena Oliveira, I. (2015). *Onychophora*. Springer, Berlin.

Mayer, G., Oliveira, I. S., Baer, A., Hammel, J. U., Gallant, J. and Hochberg, R. (2015). Capture of prey, feeding, and functional anatomy of the jaws in velvet worms (Onychophora). *Integrative and Comparative Biology*, **55**, 217–227.

McDonald, D. and Daniels, S. (2012). Phylogeography of the Cape velvet worm (Onychophora: *Peripatopsis capensis*) reveals the impact of Pliocene/Pleistocene climatic oscillations on Afromontane forest in the Western Cape, South Africa. *Journal of Evolutionary Biology*, **25**, 824–835.

Meier, R., Shiyang, K., Vaidya, G. and Ng, P. K. (2006). DNA barcoding and taxonomy in Diptera: a tale of high intraspecific variability and low identification success. *Systematic Biology*, **55**, 715–728.

Meyer, C. P. and Paulay, G. (2005). DNA barcoding: error rates based on comprehensive sampling. *PLoS Biology*, **3**, e422.

Miller, M. A., Pfeiffer, W. and Schwartz, T. (2010). Creating the CIPRES Science Gateway for inference of large phylogenetic trees in *Proceedings of the Gateway Computing Environments Workshop* (*GCE*). New Orleans, Los Angeles, USA.

Monge-Najera, J. (1995). Phylogeny, biogeography and reproductive trends in the Onychophora. *Zoological Journal of the Linnean Society*, **114**, 21–60.

Murienne, J., Daniels, S. R., Buckley, T. R., Mayer, G. and Giribet, G. (2014). A living fossil tale of Pangaean biogeography. *Proceedings of the Royal Society of London B: Biological Sciences*, **281**, 1–10.

Nei, M. and Kumar, S. (2000). *Molecular evolution and phylogenetics*. Oxford University Press, New York, USA.

New, T. (1995). Onychophora in invertebrate conservation: priorities, practice and prospects. *Zoological Journal of the Linnean Society*, **114**, 77–89.

O'Meagher, B., du Pisani, L. G. and White, D. H. (1998). Evolution of drought policy and related science in Australia and South Africa. *Agricultural Systems*, **57**, 231–258.

Oliveira, I., Wieloch, A. H. and Mayer, G. (2010). Revised taxonomy and redescription of two species of the Peripatidae (Onychophora) from Brazil: a step towards consistent terminology of morphological characters. *Zootaxa*, **2493**, 16–34.

Oliveira, I. d. S., Lacorte, G. A., Weck-Heimann, A., Cordeiro, L. M., Wieloch, A. H. and Mayer, G. (2015). A new and critically endangered species and genus of Onychophora (Peripatidae) from the Brazilian savannah–a vulnerable biodiversity hotspot. *Systematics and Biodiversity*, **13**, 211–233.

Oliveira, I. d. S. and Mayer, G. (2017). A new giant egg-laying onychophoran (Peripatopsidae) reveals evolutionary and biogeographical aspects of Australian velvet worms. *Organisms, Diversity and Evolution*, **17**, 375–391.

Oliveira, I. S., Lacorte, G. A., Fonseca, C. G., Wieloch, A. H. and Mayer, G. (2011). Cryptic speciation in Brazilian *Epiperipatus* (Onychophora: Peripatidae) reveals an underestimated diversity among the peripatid velvet worms. *PLoS ONE*, **6**, e19973.

Ou, Q., Shu, D. and Mayer, G. (2012). Cambrian lobopodians and extant onychophorans provide new insights into early cephalization in Panarthropoda. *Nature Communications*, **3**, 1261.

Park, D. S., Foottit, R., Maw, E. and Hebert, P. D. N. (2011). Barcoding bugs: DNA-based identification of the true bugs (Insecta: Hemiptera: Heteroptera). *PLoS ONE*, **6**, e18749.

Pollard, E. C. (1893). Notes on the Peripatus of Dominica. *Quaternary Journal of Microscopical Science*, **35**, 285–293.

Porter, A. H. (1999). Refugees from lost habitat and reorganization of genetic population structure. *Conservation Biology*, **13**, 850–859.

Prendini, L., Weygoldt, P. and Wheeler, W. C. (2005). Systematics of the *Damon variegatus* group of African whip spiders (Chelicerata: Amblypygi): evidence from behaviour, morphology and DNA. *Organisms, Diversity and Evolution*, **5**, 203–236.

Puillandre, N., Lambert, A., Brouillet, S. and Achaz, G. (2012). ABGD, Automatic Barcode Gap Discovery for primary species delimitation. *Molecular Ecology*, **21**, 1864–1877.

Ratnasingham, S. and Hebert, P. D. (2007). BOLD: The Barcode of Life Data System (http://www. barcodinglife. org). *Molecular Ecology Notes*, **7**, 355–364.

Read, V. S. J. (1988). The application of scanning electron microscopy to the systematics of the neotropical Peripatidae (Onychophora). *Zoological Journal of the Linnean Society*, **93**, 187–223.

Read, V. S. J. and Hughes, R. (1987). Feeding behaviour and prey choice in *Macroperipatus torquatus* (Onychophora). *Proceedings of the Royal Society of London B: Biological Sciences*, **230**, 483–506.

Reid, A. (1996). Review of the Peripatopsidae (Onychophora) in Australia, with comments on peripatopsid relationships. *Invertebrate Systematics*, **10**, 663–936.

Reid, A. (2002). Western Australian Onychophora (Peripatopsidae): a new genus, *Kumbadjena*, for a southern species-complex. *Records of the Western Australian Museum*, **21**, 129–156.

Reid, A. L. (2000). Descriptions of *Lathropatus nemorum.* gen. et sp. nov., and six new *Ooperipatus* Dendy (Onychophora: Peripatopsidae) from south-eastern Australia. *Proceedings of the Royal Society of Victoria*, **112**, 153–184.

Reid, A. L., Tait, N. N., Briscoe, D. A. and Rowell, D. M. (1995). Morphological, cytogenetic and allozymic variation within *Cephalofovea* (Onychophora: Peripatopsidae) with descriptions of three new species. *Zoological Journal of the Linnean Society*, **114**, 115–138.

Reinhard, J. and Rowell, D. M. (2005). Social behaviour in an Australian velvet worm, *Euperipatoides rowelli* (Onychophora: Peripatopsidae). *Journal of Zoology*, **267**, 1–7.

Rockman, M. V., Rowell, D. M. and Tait, N. N. (2001). Phylogenetics of *Planipapillus*, lawn-headed onychophorans of the Australian Alps, based on nuclear and mitochondrial gene sequences. *Molecular Phylogenetics and Evolution*, **21**, 103–116.

Rowell, D. M., Higgins, A. V., Briscoe, D. A. and Tait, N. N. (1995). The use of chromosomal data in the systematics of viviparous onychophorans from Australia (Onychophora: Peripatopsidae). *Zoological Journal of the Linnean Society*, **114**, 139–153.

Ruhberg, H. and Daniels, S. R. (2013). Morphological assessment supports the recognition of four novel species in the widely distributed velvet worm *Peripatopsis moseleyi sensu lato* (Onychophora : Peripatopsidae). *Invertebrate Systematics*, **27**, 131–145.

Schulmeister, S. (2003). Simultaneous analysis of basal Hymenoptera (Insecta): introducing robust-choice sensitivity analysis. *Biological Journal of the Linnean Society*, **79**, 245–275.

Sharma, P. and Giribet, G. (2009). Sandokanid phylogeny based on eight molecular markers–the evolution of a southeast Asian endemic family of Laniatores (Arachnida, Opiliones). *Molecular Phylogenetics and Evolution*, **52**, 432–447.

Soltis, P. S. and Soltis, D. E. (2003). Applying the bootstrap in phylogeny reconstruction. *Statistical Science*, **18**, 256–267.

Stamatakis, A. (2014). RAxML version 8: a tool for phylogenetic analysis and post-analysis of large phylogenies. *Bioinformatics*, **30**, 1312–1313.

Storch, V. and Ruhberg, H. (1977). Fine structure of the sensilla of *Peripatopsis moseleyi* (Onychophora). *Cell and Tissue Research*, **177**, 539–553.

Storch, V. and Ruhberg, H. (1993). Onychophora. *Microscopic Anatomy of Invertebrates*, **12**, 11–56.

Strausfeld, N. J., Hansen, L., Li, Y., Gomez, R. S. and Ito, K. (1998). Evolution, discovery, and interpretations of arthropod mushroom bodies. *Learning and Memory*, **5**, 11–37.

Sunnucks, P. and Wilson, A. (1999). Microsatellite markers for the onychophoran *Euperipatoides rowelli*. *Molecular Ecology*, **8**, 899–900.

Tait, N. and Briscoe, D. (1990). Sexual head structures in the Onychophora: unique modifications for sperm transfer. *Journal of Natural History*, **24**, 1517–1527.

Tait, N. and Briscoe, D. (1995). Genetic differentiation within New Zealand Onychophora and their relationships to the Australian fauna. *Zoological Journal of the Linnean Society*, **114**, 103–113.

Tait, N. N. and Norman, J. M. (2001). Novel mating behaviour in *Florelliceps stutchburyae* gen. nov., sp. nov. (Onychophora: Peripatopsidae) from Australia. *Journal of Zoology*, **253**, 301–308.

Thompson, J. D., Higgins, D. G. and Gibson, T. J. (1994). CLUSTAL W: improving the sensitivity of progressive multiple sequence alignment through sequence weighting, position-specific gap penalties and weight matrix choice. *Nucleic Acids Research*, **22**, 4673–4680.

Trewick, S. (1999). Molecular diversity of Dunedin peripatus (Onychophora: Peripatopsidae). *New Zealand Journal of Zoology*, **26**, 381–393.

Trewick, S. (2000). Mitochondrial DNA sequences support allozyme evidence for cryptic radiation of New Zealand Peripatoides (Onychophora). *Molecular Ecology*, **9**, 269–281.

Trewick, S. A. (1998). Sympatric cryptic species in New Zealand Onychophora. *Biological Journal of the Linnean Society*, **63**, 307–329.

Walker, M. H. and Tait, N. N. (2004). Studies of embryonic development and the reproductive cycle in ovoviviparous Australian Onychophora (Peripatopsidae). *Journal of Zoology*, **264**, 333–354.

Wiemers, M. and Fiedler, K. (2007). Does the DNA barcoding gap exist? –a case study in blue butterflies (Lepidoptera: Lycaenidae). *Frontiers in Zoology*, **4**, 8.

Zhang, D. X. and Hewitt, G. (1997). Assessment of the universality and utility of a set of conserved mitochondrial COI primers in insects. *Insect Molecular Biology*, **6**, 143–150.

APPENDICES

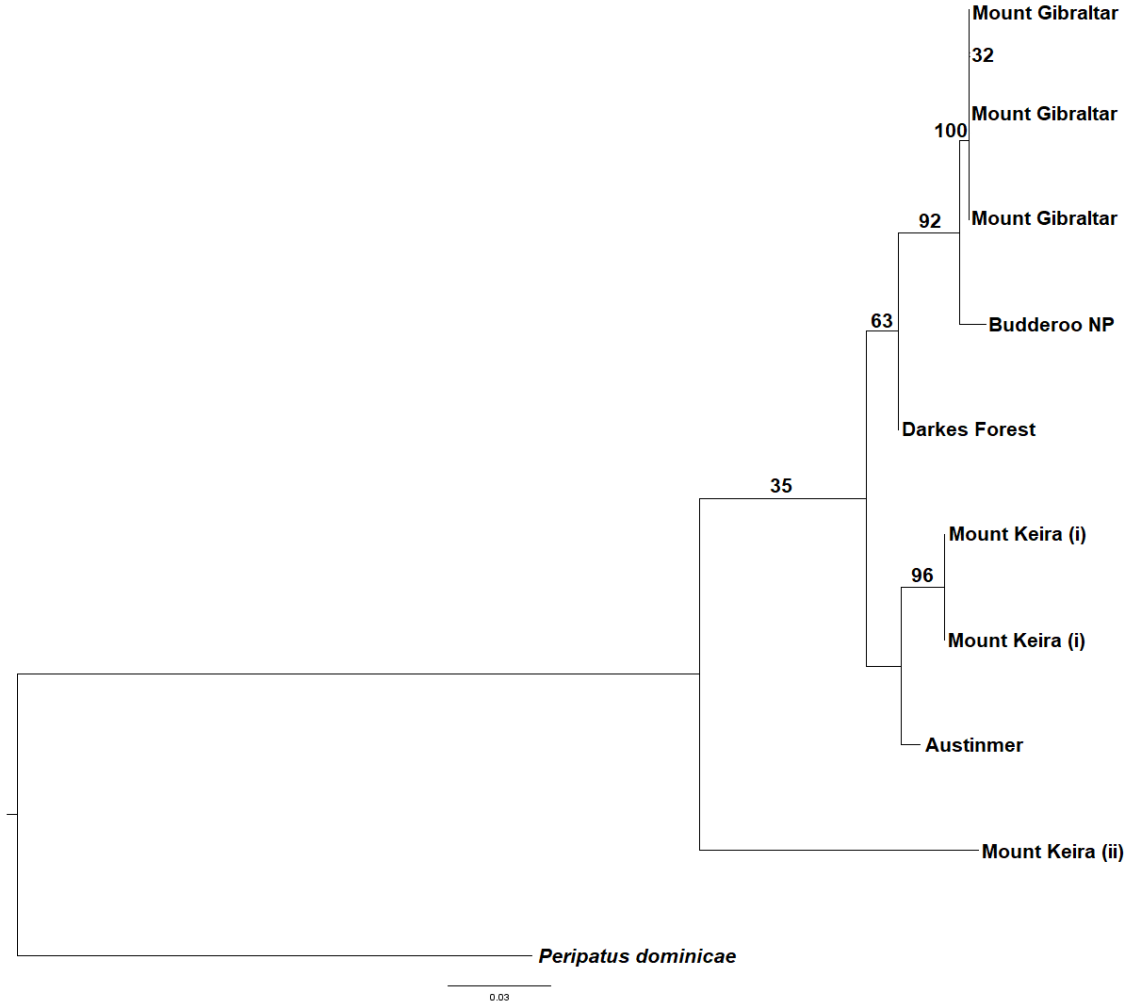

Appendix 1. Phylogenetic relationships among specimens examined, using only the 'barcode' region sequences, including the outgroup, Peripatus dominicae. Maximum Likelihood tree constructed from COI nucleotide sequences. Node labels indicate bootstrap support. Bootstrap iterations = 500.

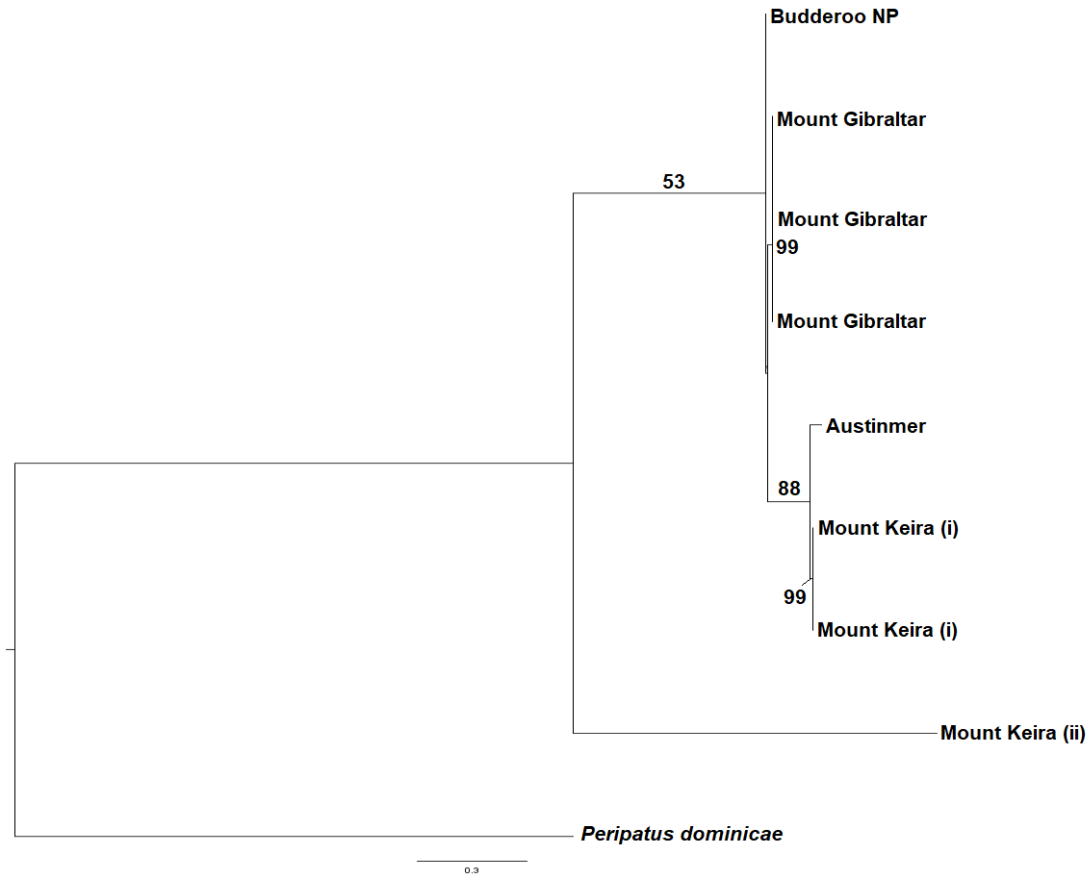

Appendix 2. Phylogenetic relationships among specimens examined, using only the sequences with both the 'barcode' and 'fragment 3', including the outgroup, Peripatus dominicae. Maximum Likelihood tree constructed from COI nucleotide sequences. Node labels indicate bootstrap support. Bootstrap iterations = 500.

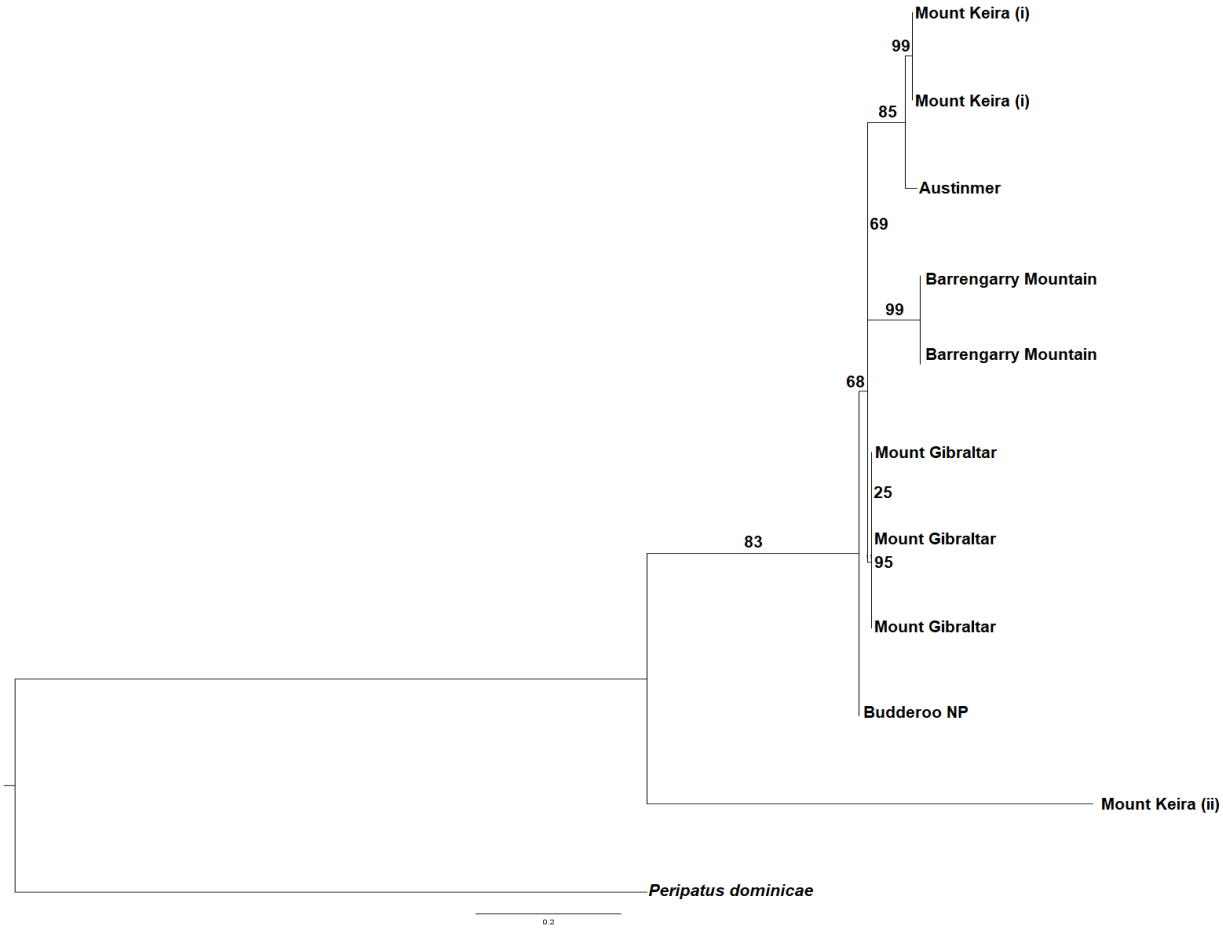

Appendix 3. Phylogenetic relationships among specimens examined, using only 'fragment 3', including the outgroup, Peripatus dominicae. Maximum Likelihood tree constructed from COI nucleotide sequences. Node labels indicate bootstrap support. Bootstrap iterations = 500.

Mt Gibraltar

Material examined. 5 ♂, 6 ♀, Mount Gibraltar Nature Reserve, NSW, Australia, 34°28’0.8” S 150°25’50.4” E, 850 m (AM.CC5).

Antennal Rings. 30 rings in total; each with a single row of bristles (Fig. 7a, b).

Body colour and pattern. Light transverse patches that convex posteriorly; sometimes base pigments are tannish and brown or bluish and black; pattern less obvious in darker specimens. Pattern and pigmentations present in both sexes. Primary papillae ribbed basally and distally, papillar scales not fused (Character 3, Fig. 21a, b).

Crural glands. Ribbed basal papillar scales; smooth, narrow lip-shaped opening (Character 2, Fig. 13a, b).

Female reproductive tract. Ovoviviparous, embryos in late stages of development in individual uteri; visible pigments.

Genital opening. Low, rounded, not markedly protuberant; composed of large partially fused papillae (Character 1, Fig. 14a, b).

Male reproductive tract and associated glands. Anterior accessory glands elongated, lying freely within body cavity; gland profusely irregular with numerous twists and bends. Externally, anterior accessory glands possess ribbed papillar scales with a smooth, broad, lip-shaped distal opening (Character 1, Fig. 8a, b). Posterior accessory glands elongated, with distal tip folded. Vasa efferntia walls thin and white, almost transparent. Vas deferens walls white and opaque, loops posteriorly towards ejector tract.

Measurements. HWE males 1.1 mm (n = 5). HWE females 1.5 mm (n = 6).

Nephridiopore. Smooth distal openings, distal tip sometimes folded, ribbed basally (Character 1, Fig. 16a, b).

Austinmer

Material examined. 1 ♂, Austinmer, NSW, Australia, 34°17’51.0” S, 150°55’55” E, 132 m, (AM.CC3).

Antennal Rings. 30 rings in total; each with a single row of bristles (Fig. 7a, b).

Body colour and pattern. Light transverse patches that convex posteriorly; base pigments are tannish and brown. Primary papillae have smooth, partly fused distal papillar scales. Basal papillar scales are ribbed. (Character 1, Fig. 19a, b).

Crural glands. Not present in female specimen.

Female reproductive tract. Ovoviviparous, embryos in late stages of development in individual uteri; visible pigments.

Genital opening. Low, rounded, not markedly protuberant composed of large partially fused papillae (Character 1, Fig. 14a, b).

Male reproductive tract and associated glands. No male specimens available.

Measurements. HWE female 1.2 mm (n = 1).

Nephridiopore. Smooth distal opening; ribbed basally (Character 1, Fig. 16a, b).

Barrengarry Mountain

Material examined. 2♂, 3♀, Barrengarry Mountain, NSW, Australia, 34°41’08” S, 150°29’52” E, 504 m, (AM KS.119221).

Antennal Rings. 30 rings in total; each with a single row of bristles (Fig. 7a, b).

Body colour and pattern. Light transverse patches that convex posteriorly; sometimes base pigments are tannish and brown. Pattern and pigmentations present in both sexes. Primary distal papillar scales papillose, sometimes fused; basal papillar scales ribbed. (Character 2, Fig. 20).

Crural glands. Ribbed papillar scales basally; smooth, narrow, lip-shaped distal opening (Character 2, Fig. 13a, b).

Female reproductive tract. No embryos observed in uteri.

Genital opening. Low, rounded, not markedly protuberant; composed of large partially fused papillae (Character 1, Fig. 14a, b).

Male reproductive tract and associated glands. Anterior accessory glands elongated, lying freely within body cavity; absence of irregularities such as curves or bends. Externally, anterior accessory glands have ribbed papillar scales with a smooth, broad, lip-shaped distal opening. (Character 4, Fig. 11a, b). Posterior accessory glands elongated, with distal tip folded. Vasa efferntia walls thin and white, almost transparent. Vas deferens walls white and opaque, loops posteriorly towards ejector tract.

Measurements. HWE males 1 mm (n = 2). HWE females 1.1 mm (n = 3).

Nephridiopore. Smooth distal openings, distal tip sometimes folded, ribbed basally. (Character 2, Fig. 17a, b).

Macquarie Pass National Park

Material examined. 2♂, 2♀, Macquarie Pass National Park, NSW, Australia, 34°34’0.0” S, 150°39’0.0” E, 520m, (AM KS.045948).

Antennal Rings. 30 rings in total; each with a single row of bristles (Fig. 7a, b).

Body colour and pattern. Light transverse patches that convex posteriorly; sometimes base pigments are tannish and brown. Pattern and pigmentations present in both sexes. Primary distal and basal papillar scales ribbed, and not fused (Character 3, Fig 21a, b).

Crural glands. Ribbed papillar scales basally, smooth, narrow, lip-shaped distal opening (Character 2, Fig. 13a, b).

Female reproductive tract. Ovoviviparous, embryos in late stages of development in individual uteri; no visible pigments.

Genital opening. Low, rounded, not markedly protuberant; composed of large partially fused papillae (Character 1, Fig. 14a, b).

Male reproductive tract and associated glands. Anterior accessory glands elongated, lying freely within body cavity; absence of irregularities such as curves or bends. Externally, anterior accessory glands possess fused ribbed papillar scales, ribbed distal opening (Character 3, Fig. 10a, b). Posterior accessory glands elongated, with distal tip folded. Vasa efferntia walls thin and white, almost transparent. Vas deferens walls white and opaque, loops posteriorly towards ejector tract.

Measurements. HWE males 0.9 mm (n = 2). HWE females 1.4 mm (n = 2).

Nephridiopore. Smooth distal openings, distal tip sometimes folded, ribbed basally (Character 1, Fig. 16a, b).

Darkes Forest

Material examined. 2♂, 2♀, Darkes Forest, NSW, Australia, 34°12’0.0” S, 150°55’0.0” E, 337 m, (AM KS.91348).

Antennal Rings. 30 rings in total; each with a single row of bristles (Fig. 7a, b).

Body colour and pattern. Light transverse patches that convex posteriorly; sometimes base pigments are tannish and brown or bluish and black; pattern less obvious in darker specimens. Pattern and pigmentations present in both sexes. Primary distal papillar scales crenulated; basal papillar scales ribbed (Character 4, Fig. 22a, b).

Crural glands. Ribbed papillar scales basally; smooth, narrow, lip-shaped distal opening (Character 2, Fig. 13a, b).

Female reproductive tract. Ovoviviparous, embryos in late stages of development in individual uteri; visible pigments.

Genital opening. Low, rounded, not markedly protuberant; composed of large partially fused papillae (Character 1, Fig. 14a, b).

Male reproductive tract and associated glands. Anterior accessory glands elongated, lying freely within body cavity; absence of irregularities such as curves or bends. Externally, anterior accessory glands possess ribbed papillar scales with a smooth, broad, lip-shaped distal opening (Character 1, Fig. 8a, b). Posterior accessory glands elongated, with distal tip folded. Vasa efferntia walls thin and white, almost transparent. Vas deferens walls white and opaque, loops posteriorly towards ejector tract.

Measurements. HWE males 1.2 mm (n = 2). HWE females 1.7 mm (n = 2).

Nephridiopore. Smooth distal openings, distal tip sometimes folded; ribbed basally (Character 1, Fig. 16a, b).

Budderoo National Park

Material examined. 2♀, Budderoo National Park, NSW, Australia, 34°38’02” S, 150°43’37” E, 151 m (AM KS.119248).

Antennal Rings. 30 rings in total; each with a single row of bristles (Fig. 7a, b).

Body colour and pattern. Light transverse patches that convex posteriorly; base pigments are tannish and brown. Primary distal papillar scales smooth and partially fused; basal papillar scales ribbed (Character 1, Fig. 19a, b).

Crural glands. Not present in female specimens.

Female reproductive tract. No embryos observed in uteri.

Genital opening. Papillae discrete, less fused, with long spines (Character 2, Fig. 15).

Male reproductive tract and associated glands. No male specimens available.

Measurements. HWE females 1.1 mm (n = 2).

Nephridiopore. Could not be determined (structure inverted).

Mt Keira

Material examined. 1♂, NSW, Australia, 34°24’4.0” S, 150°50’39.1” E, 333 m (AM.CC).

Antennal Rings. 30 rings in total; each with a single row of bristles (Fig. 7a, b).

Body colour and pattern. Transverse patches that convex posteriorly; base pigments are tannish and brown; pattern less obvious due to darker pigments. Primary papillar scales smooth and partially fused; basal papillar scales ribbed (Character 1, Fig. 19a, b).

Crural glands. Ribbed papillar scales basally, distal half smooth with long slit-like distal opening (Character 1, Fig. 12a, b).

Female reproductive tract. No female specimens available.

Genital opening. Low, rounded, not markedly protuberant composed of large partially fused papillae (Character 1, Fig. 14a, b).

Male reproductive tract and associated glands. Anterior accessory glands elongated, lying freely within body cavity; absence of irregularities such as curves or bends. Externally, anterior accessory glands possess ribbed papillar scales with a smooth, broad, lip-shaped distal opening (Character 1, Fig. 8a, b). Posterior accessory glands elongated, with distal tip folded. Vasa efferntia walls thin and white, almost transparent. Vas deferens walls white and opaque, loops posteriorly towards ejector tract.

Measurements. HWE male 1 mm (n = 1).

Nephridiopore. Smooth distal openings, distal tip folded, ribbed basally (Character 1, Fig. 16a, b).

Heathcote

Material examined. 1♂, Heathcote, NSW, Australia, 34°05’5.2” S, 151°01’28.8” E, 200 m (AM.CC1).

Antennal Rings. 30 rings in total; each with a single row of bristles (Fig. 7a, b).

Body colour and pattern. Base pigments are bluish and black; pattern less obvious due to darker pigments. Primary distal and basal papillar scales ribbed, and not fused (Character 3, Fig. 21a, b).

Crural glands. Ribbed papillar scales basally, smooth, narrow, lip-shaped distal opening (Character 1, Fig. 12a, b).

Female reproductive tract. No female specimens available.

Genital opening. Low, rounded, not markedly protuberant composed of large partially fused papillae (Character 1, Fig. 14a, b).

Male reproductive tract and associated glands. Anterior accessory glands elongated, lying freely within body cavity; absence of irregularities such as curves or bends. Externally, anterior accessory glands possess ribbed papillar scales with a smooth, narrow, lip-shaped distal opening (Character 2, Fig. 9a, b). Posterior accessory glands elongated, with distal tip folded. Vasa efferntia walls thin and white, almost transparent. Vas deferens walls white and opaque, loops posteriorly towards ejector tract.

Measurements. HWE male 1.1 mm (n = 1).

Nephridiopore. Smooth, inconspicuous U-shaped opening (Character 3, Fig. 18).

Royal National Park

Material examined. 1 ♀, Royal National Park, NSW, Australia, 34°09’6.9” S, 151°00’51.4” E, 138 m (AM.CC2).

Antennal Rings. 30 rings in total; each with a single row of bristles (Fig. 7a, b).

Body colour and pattern. Light transverse patches that convex posteriorly; base pigments are tannish and brown. Primary distal primary papillar scales smooth, or only slightly papillose, and partially fused; basal primary papillar scales ribbed (Character 1, Fig. 19a, b).

Crural glands. No male specimens available.

Female reproductive tract. No embryos observed in uteri

Genital opening. Low, rounded, not markedly protuberant composed of large partially fused papillae around X-shaped opening (Character 1, Fig. 14a, b).

Male reproductive tract and associated glands. No male specimens available.

Measurements. HWE female 1.5 mm (n = 1).

Nephridiopore. Smooth distal openings, distal tip sometimes folded, ribbed basally. (Character 1, Fig. 16a, b).

Bundanoon

Material examined. 3♂, 2♀, Bundanoon, NSW, Australia, 34°40’31.5” S, 150°16’51.9” E, 674 m (AM KS.16580).

Antennal Rings. 30 rings in total; each with a single row of bristles (Fig. 7a, b).

Body colour and pattern. Light transverse patches that convex posteriorly; sometimes base pigments are tannish and brown or bluish and black; pattern less obvious in darker specimens. Pattern and pigmentations present in both sexes. Distal primary papillar scales ribbed basally, ribs partially fused distally, appear crenulated (Character 4, Fig. 22a, b).

Crural glands. Ribbed papillar scales basally, distal half smooth with long slit-like distal opening (Character 1, Fig. 12a, b).

Female reproductive tract. Ovoviviparous, embryos in late stages of development in individual uteri; visible pigments.

Genital opening. Low, rounded, not markedly protuberant composed of large partially fused papillae around X-shaped opening (Character 1, Fig. 14a, b).

Male reproductive tract and associated glands. Anterior accessory glands elongated, lying freely within body cavity; absence of irregularities such as curves or bends. Externally, anterior accessory glands possess ribbed papillar scales with a smooth, broad, lip-shaped distal opening (Character 1, Fig. 8a, b). Posterior accessory glands elongated, with distal tip folded. Vasa efferntia walls thin and white, almost transparent. Vas deferens walls white and opaque, loops posteriorly towards ejector tract.

Measurements. HWE males 1.5 mm (n = 3). HWE females 2 mm (n = 2).

Nephridiopore. Smooth distal openings, distal tip sometimes folded, ribbed basally (Character 1, Fig. 16a, b).

Twin Falls

Material examined. 3♂, 2♀, Twin Falls, NSW, Australia, 34°23’42.0” S, 150°16’48.0” E, 677 m (AM KS.28191).

Antennal Rings. 30 rings in total; each with a single row of bristles (Fig. 7a, b).

Body colour and pattern. Light transverse patches that convex posteriorly; sometimes base pigments are tannish and brown or bluish and black; pattern less obvious in darker specimens. Pattern and pigmentations present in both sexes. Distal primary papillar scales ribbed basally, ribs partially fused distally, appear crenulated (Character 4, Fig. 22a, b).

Crural glands. Ribbed papillar scales basally, distal half smooth with long slit-like distal opening (Character 1, Fig. 12a, b).

Female reproductive tract. Ovoviviparous, embryos in late stages of development in individual uteri; visible pigments.

Genital opening. Low, rounded, not markedly protuberant composed of large partially fused papillae around X-shaped opening (Character 1, Fig. 14a, b).

Male reproductive tract and associated glands. Anterior accessory glands elongated, lying freely within body cavity; absence of irregularities such as curves or bends. Externally, anterior accessory glands possess ribbed papillar scales with a smooth, broad, lip-shaped distal opening (Character 1, Fig. 8a, b). Posterior accessory glands elongated, with distal tip folded. Vasa efferntia walls thin and white, almost transparent. Vas deferens walls white and opaque, loops posteriorly towards ejector tract.

Measurements. HWE males 1.3 mm (n = 3). HWE females 1.9 mm (n = 2).

Nephridiopore. Smooth distal openings, distal tip sometimes folded, ribbed basally. (Character 1, Fig. 16a, b).

Avoca

Material examined. 3♂, 2♀, Avoca, NSW, Australia, 34°37'0.0" S, 150°29'1.0" E, 714 m (AM KS.28199).

Antennal Rings. 30 rings in total; each with a single row of bristles (Fig. 7a, b).

Body colour and pattern. Light transverse patches that convex posteriorly; sometimes base pigments are tannish and brown or bluish and black; pattern less obvious in darker specimens. Pattern and pigmentations present in both sexes. Distal primary papillar scales ribbed basally, ribs partially fused distally, appear crenulated (Character 4, Fig. 22a, b).

Crural glands. Ribbed papillar scales basally, distal half smooth with long slit-like distal opening (Character 1, Fig. 12a, b).

Female reproductive tract. Ovoviviparous, embryos in late stages of development in individual uteri; visible pigments.

Genital opening. Low, rounded, not markedly protuberant composed of large partially fused papillae around X-shaped opening (Character 1, Fig. 14a, b).

Male reproductive tract and associated glands. Anterior accessory glands elongated, lying freely within body cavity; absence of irregularities such as curves or bends. Externally, anterior accessory glands possess ribbed papillar scales with a smooth, broad, lip-shaped distal opening (Character 1, Fig. 8a, b). Posterior accessory glands elongated, with distal tip folded. Vasa efferntia walls thin and white, almost transparent. Vas deferens walls white and opaque, loops posteriorly towards ejector tract.

Measurements. HWE males 1.4 mm (n = 3). HWE females 1.9 mm (n = 2).

Nephridiopore. Broad fan-like nephridiopore. Rim smooth on proximal - towards base of oncopod or distal margin only (Character 2, Fig. 13a, b).